nature communications

Article

https://doi.org/10.1038/s41467-025-68086-5

Calcium channel blockers increase the risk of aortic aneurysm and dissection

Received: 12 May 2025

Accepted: 16 December 2025

Published online: 25 December 2025

Check for updates

Tianfeng Ma[1,8], Zeyu Cai[2,8], Xinming Xu[3,8], Long Cao[1,4,8], Ao Wang[2], Zhongshuang Zhang[2], Siting Zhang[2], Zhenkun Huang[2], Jingjing Luo[5], Sen Lin[2], Jiashu Ge[1], Xinhao Wang[1], Yi Fu[2], Fang Yu[2], Jing Zhou[2], Lixin Wang[6,7], Hongpeng Zhang[1], Xiang Gao[3,9] ✉, Wei Guo[1,9] ✉ & Wei Kong[2] ✉

Aortic aneurysm and dissection (AAD) are life-threatening conditions without effective medications. Impaired contractility of vascular smooth muscle cells (VSMCs) is strongly linked to AAD, but the role of calcium channel blockers (CCBs), which directly inhibits VSMC contractility, in AAD remains unclear. Here we showed data from 501,878 initially AAD-free participants in UK Biobank. Over a median follow-up of 13.5 years, CCB users had higher AAD risk (HR = 1.31) than hypertensive patients not receiving antihypertensive treatment. In mouse models of AAD, CCBs significantly aggravated aortic stiffness and AAD development. For patients with type B aortic dissection who underwent endovascular repair, CCBs limited AAD regression compared with other antihypertensives. Moreover, silencing of protein kinase cGMP-dependent 1 (PRKG1) significantly mitigated CCB-aggravated AAD progression. These findings suggest that CCBs may increase AAD risk and post-stent surgery prognosis, highlighting the need for caution when prescribing CCBs to hypertensive patients at risk for AAD.

Aortic aneurysm and dissection (AAD) are life-threatening cardiovascular conditions associated with high mortality rates. Aortic aneurysm refers to the irreversible enlargement of the aorta, resulting in a diameter exceeding 1.5 times that of adjacent normal vessels. Aortic dissection is defined as disruption of the intima leading to separation of the aortic wall layers followed by the formation of a false lumen[1]. Depending on the location, AAD are classified into thoracic aortic aneurysm/dissection (TAAD) and abdominal aortic aneurysm (AAA)[2,3]. Although recognized as distinct disease entities, TAAD and AAA share common pathological changes, including vascular extracellular matrix degradation, inflammation, and dysfunction of vascular smooth muscle cells (VSMCs). Currently, the management of AAD relies solely on surgical intervention, including artificial blood vessel replacement and endovascular stent graft repair[4]. However, at present, only β-blockers or angiotensin II receptor blockers (ARBs) are recommended for aortic aneurysms in patients with Marfan syndrome. There are currently no proven drugs to prevent the occurrence of or slow the expansion of the aorta in patients with non-hereditary AAD, including blood pressure-lowering drugs[5–7], lipid-modifying medications[8], anti-inflammatory or antibiotics drugs[9–11], anti-thrombotic drugs[12].

Hypertension has long been recognized as an independent risk factor for AAD[13,14]. In clinical practice, antihypertensive drugs,

[1]Department of Vascular and Endovascular Surgery, Chinese PLA General Hospital, Beijing, China. [2]Department of Physiology and Pathophysiology, School of Basic Medical Sciences, Peking University; State Key Laboratory of Vascular Homeostasis and Remodeling, Peking University, Beijing, China. [3]Department of Nutrition and Food Hygiene, School of Public Health, Institute of Nutrition, Fudan University, Shanghai, China. [4]Department of General Surgery, The 983rd Hospital of Joint Logistic Support Force of PLA, Tianjin, China. [5]Department of Cardiovascular Surgery, Union Hospital, Tongji Medical College, Huazhong University of Science and Technology, Wuhan, China. [6]Department of Vascular Surgery, Zhongshan Hospital, Fudan University; Vascular Surgery Institute of Fudan University, Shanghai, China. [7]Xiamen municipal Vascular Disease Precise Diagnose & Treatment Lab, Xiamen, China. [8]These authors contributed equally: Tianfeng Ma, Zeyu Cai, Xinming Xu, Long Cao. [9]These authors jointly supervised this work, Xiang Gao, Wei Guo, Wei Kong.
✉e-mail: xiang_gao@fudan.edu.cn; guoweiplagh@sina.com; kongw@bjmu.edu.cn

https://doi.org/10.1038/s41467-025-68086-5

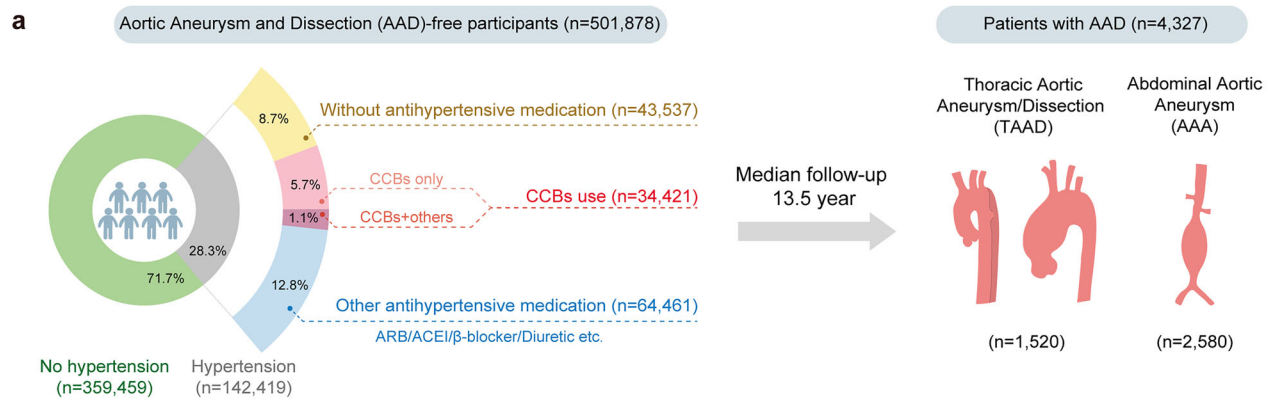

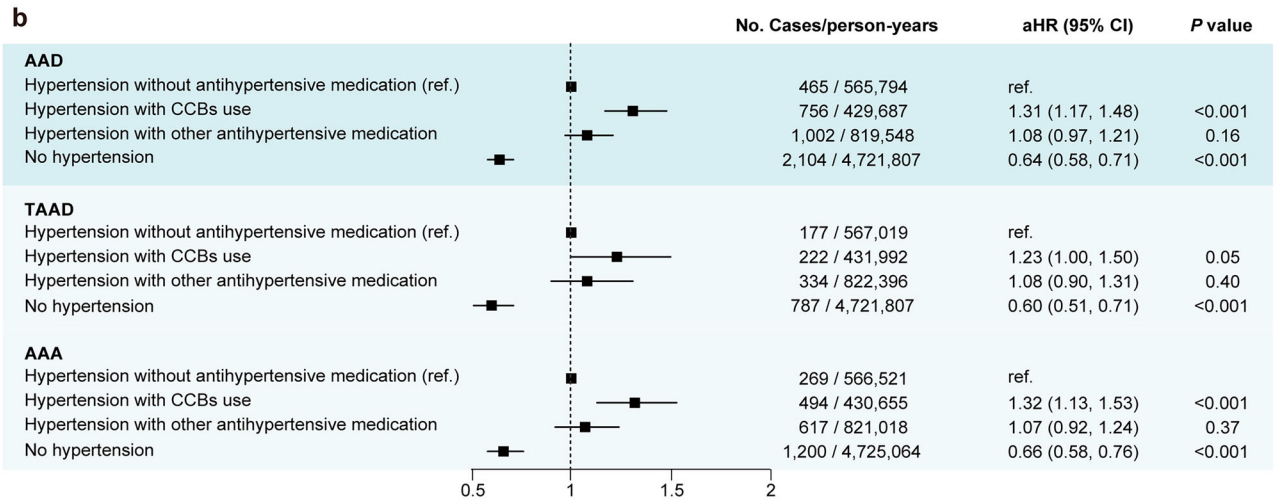

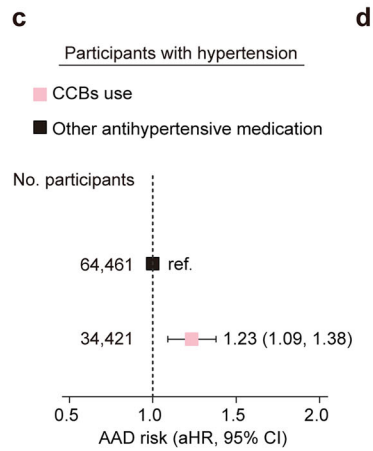

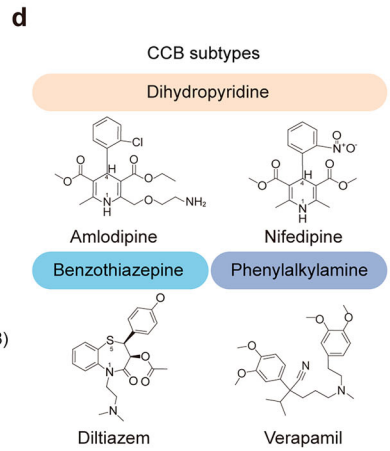

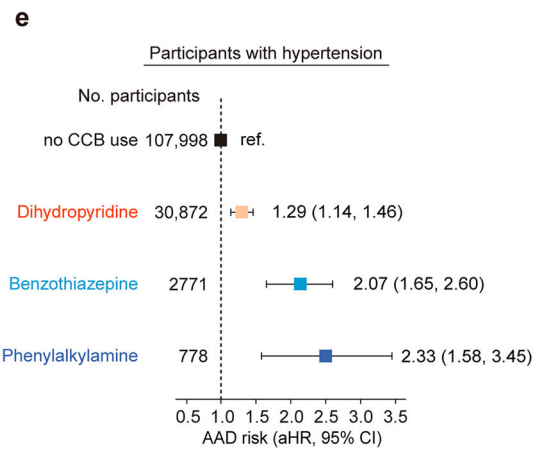

including angiotensin II receptor blockers (ARBs), calcium channel blockers (CCBs), and β-blockers, are commonly prescribed to AAD patients to reduce pressure on the aortic wall, but the effect of various antihypertensive drugs on AAD patients remains unclear. Notably, emerging evidence indicates that the development of AAD is attributed to the impaired VSMC contractility[15]. Reduced expression of contractile apparatus proteins (e.g., myosin heavy chain [MYH11], smooth muscle α-actin [SM α-actin], and smooth muscle protein 22-α [SM22-α]) is observed in the aortas of patients with TAAD and AAA[16]. Additionally, genetic mutations in myosin heavy chain 11 (*MYH11*), actin α 2 (*ACTA2*), myosin light chain kinase (*MYLK*), and cGMP-dependent protein kinase type I (*PRKG1*) are linked to TAAD[17,18]. Moreover, patients with AAD have shown reduced vascular contractility, accompanied by changes in mechanical properties, such as increased stiffness[19–21]. This raises concerns about whether antihypertensive drugs that inhibit VSMC contractility, such as CCBs[22], pose potential risks to AAD onset. Previous studies have reported that CCBs (amlodipine, diltiazem, and azelnidipine), at doses 5–10 times higher than clinical doses, may alleviate angiotensin II (AngII)-induced AAD formation when co-administered with AngII in mice[23–26]. However, a single study revealed that amlodipine and verapamil promoted aorta expansion in mice with Marfan syndrome (MFS)[27]. Furthermore, in a randomized controlled trial involving 224 patients with small AAAs, amlodipine failed to delay aortic expansion[7]. Currently, however, all clinical studies have focused on the medication treatment of patients with diagnosed AAD, while the impact of CCB use in hypertensive patients on the incidence of AAD remains unclear.

Fig. 1 | CCBs use and AAD/AAD subtypes risks in the UKB. a Overview of the included AAD-free participants from the UKB (n = 501,878). Pie chart showed the exposure groups categorized by hypertension and antihypertensive medications in relation to the total number of included participants. **b** Association of hypertension status and antihypertensive medication use (CCBs or other antihypertensive medication excluding CCBs use) with AAD/AAD subtypes risks among the AAD-free UKB participants (n = 501,878). Adjusted HRs of AAD/AAD subtypes risks were calculated via Cox model adjusted for age (years), sex (men; women), BMI (kg/m^2), total cholesterol (mmol/L), triglycerides (mmol/L), smoking status (never; previous; current), education (College or University degree; A levels or equivalent; O levels or equivalent; None of the above), ethnicity (white; or others), and systolic blood pressure (mmHg). Squares represented HRs and error bars represented 95% CIs. The dashed line indicated the reference line (HR = 1.0). All statistical tests were two-sided, and no adjustments were made for multiple comparisons. **c** Association of CCBs with AAD risk among participants with hypertension and any antihypertensive medication use (n = 98,882, including 34,421 participants with hypertension using CCBs and 64,461 participants with hypertension using other antihypertensive medication use except for CCBs). Adjusted HR of AAD risk was calculated via Cox model adjusted for age (years), sex (men; women), BMI (kg/m2), total cholesterol (mmol/L), triglycerides (mmol/L), smoking status (never; previous; current), education (College or University degree; A levels or equivalent; O levels or equivalent; None of the above), ethnicity (white; or others), and systolic blood pressure (mmHg). Squares represented HRs and error bars represented 95% CIs. The dashed line indicated the reference line (HR = 1.0). All statistical tests were two-sided, and no adjustments were made for multiple comparisons. **d** Subtypes and chemical structures of CCBs. **e** Association of CCBs subtypes use with AAD risk among the UKB participants with hypertension (n = 142,419). Adjusted HRs of AAD risk were calculated via Cox model adjusted for age (years), sex (men; women), BMI (kg/m^2), total cholesterol (mmol/L), triglycerides (mmol/L), smoking status (never; previous; current), education (College or University degree; A levels or equivalent; O levels or equivalent; None of the above), ethnicity (white; or others), systolic blood pressure (mmHg), and simultaneous use of other antihypertensive medications. Squares represented HRs and error bars represented 95% CIs. The dashed line indicated the reference line (HR = 1.0). All statistical tests were two-sided, and no adjustments were made for multiple comparisons. AAD Aortic aneurysm and dissection, TAAD Thoracic aortic aneurysm and dissection, AAA Abdominal aortic aneurysm, CCB, Calcium channel blocker, BMI body mass index; HR, hazard ratio; CI, confidence interval; aHR, adjusted hazard ratio; ref, reference.

In this study, our objective was to evaluate the impact of CCBs on the risk of AAD. Here we report results of (1) the association between CCBs and their subtypes with subsequent AAD occurrence, using data from the UK Biobank; and (2) the effects of CCBs on both murine models and post-stent AAD patients.

Results

Association of CCB or subtype use with the risk of AAD in UKB participants

We first analyzed the association between CCBs and the incidence of AAD using data from the UK Biobank (Fig. 1a). Among the 501,878 participants initially free of AAD, 28.3% were identified as having hypertension (Supplementary Table 1). These hypertensive participants were divided into three groups based on their medication use: 8.7% were not taking any antihypertensives, and 6.8% were using CCBs, either exclusively (5.7%) or in combination with other antihypertensive medications (1.1%). The remaining 12.8% were classified as users of antihypertensive medications other than CCBs (Supplementary Tables 2, 3). The baseline characteristics of the participants are shown in Supplementary Table 4. Hypertensive participants, regardless of medication use, were generally older, had higher body mass index (BMI), and higher systolic blood pressure (SBP) than those without hypertension. Among hypertensive groups, CCB users were older, had more men, fewer white participants, and lower total cholesterol levels than untreated individuals or those using other antihypertensive medications.

During a median follow-up period of 13.5 years, 4,327 cases of AAD were identified, including 1520 TAAD and 2580 AAA (Fig. 1a and Supplementary Table 5). As expected, participants without hypertension had significantly lower risks of AAD, TAAD, and AAA compared to those with hypertension but without antihypertensive medication (P < 0.001 for all) (Fig. 1b). We further found that participants with hypertension and concurrent CCB use had greater risks of AAD (adjusted HR = 1.31, 95% CI: 1.17–1.48), TAAD (adjusted HR = 1.23, 95% CI: 1.00–1.50), and AAA (adjusted HR = 1.32, 95% CI: 1.13–1.53) than hypertensive patients not receiving antihypertensive medication (Fig. 1b). To minimize the indication bias that medication use itself might reflect disease severity, we restricted the analyses to the participants receiving antihypertensive medications and observed that CCB users still had a significantly greater risk of AAD (HR = 1.23, 95% CI: 1.09–1.38) than other antihypertensive medication users, with consistent results in both males and females and a relatively greater effect observed in females (Fig. 1c and Supplementary Tables 6, 7). Furthermore, among the participants with prevalent AAD, CCB use was associated with increased mortality (HR = 1.52, 95% CI: 1.04–2.21) (Supplementary Table 8).

CCBs are generally divided into three main subtypes based on their chemical structure and action mechanisms: dihydropyridines, benzothiazepines and phenylalkylamines[28](Fig. 1d). All subtypes of CCBs were associated with a significantly greater AAD risk than no CCB use among participants with hypertension, with phenylalkylamine CCBs presenting the highest risk (HR = 2.33, 95% CI: 1.58–3.45), benzothiazepine CCBs showing an intermediate risk (HR = 2.07, 95% CI: 1.65–2.60), and dihydropyridine CCBs having a relatively lower risk (HR = 1.29, 95% CI: 1.14–1.46), after further adjusting for concurrent use of other blood pressure medications (Fig. 1e). Sensitivity analysis considering the competing risk of death, using a broader definition of hypertension, excluding participants with coronary artery diseases, adjusting for eGFR, or removing participants with hypertension who used both CCBs and other antihypertensive medications yielded similar results, supporting the robustness of our study (Supplementary Tables 9–13).

CCBs aggravated both thoracic and abdominal aortic aneurysm formation in AngII-infused mouse model

We next investigated the causal effect of different CCB subtypes on the development of aortic aneurysms in an angiotensin II (AngII)-infused mouse model (Fig. 2a). Sixteen-week-old C57BL/6 J mice were subcutaneously infused with AngII (1000 ng/kg·min^{-1}) via minipumps for a total of 28 days. First, 70 sixteen-week-old male C57BL/6 J mice were initially infused with AngII for 7 days to induce hypertension. During this period, 11 mice either died of aneurysm rupture or were diagnosed with aortic aneurysm via ultrasound. Then, the remaining 59 hypertensive mice were randomly assigned to receive either a vehicle or one of four CCBs: amlodipine (1 mg/kg/day), nifedipine (20 mg/kg/day), diltiazem (8 mg/kg/day) or verapamil (12 mg/kg/day) (Supplementary Fig. 1a). Saline-infused mice were treated with vehicle and served as a negative control. As expected, all four CCB treatments significantly reduced SBP in the AngII-infused mice (Fig. 2b).

During CCB administration, we performed weekly ultrasound to monitor the diameters of the thoracic aorta (aortic root, ascending aorta, and aortic arch). Compared with those in AngII+Vehicle group, the mice in the CCB groups exhibited significant aortic expansion after 14 days of treatment, which persisted for 21 days. The AngII+verapamil group presented the largest thoracic aortic diameter among the CCB groups (AngII+verapamil *vs.* AngII+vehicle; Aortic root, 2.72 ± 0.10 *vs.* 2.18 ± 0.04 mm, P = 0.006; Ascending aorta, 2.25 ± 0.12 *vs.* 1.76 ± 0.02 mm, P = 0.043; Aortic arch, 1.93 ± 0.05 *vs.* 1.64 ± 0.02 mm,

https://doi.org/10.1038/s41467-025-68086-5

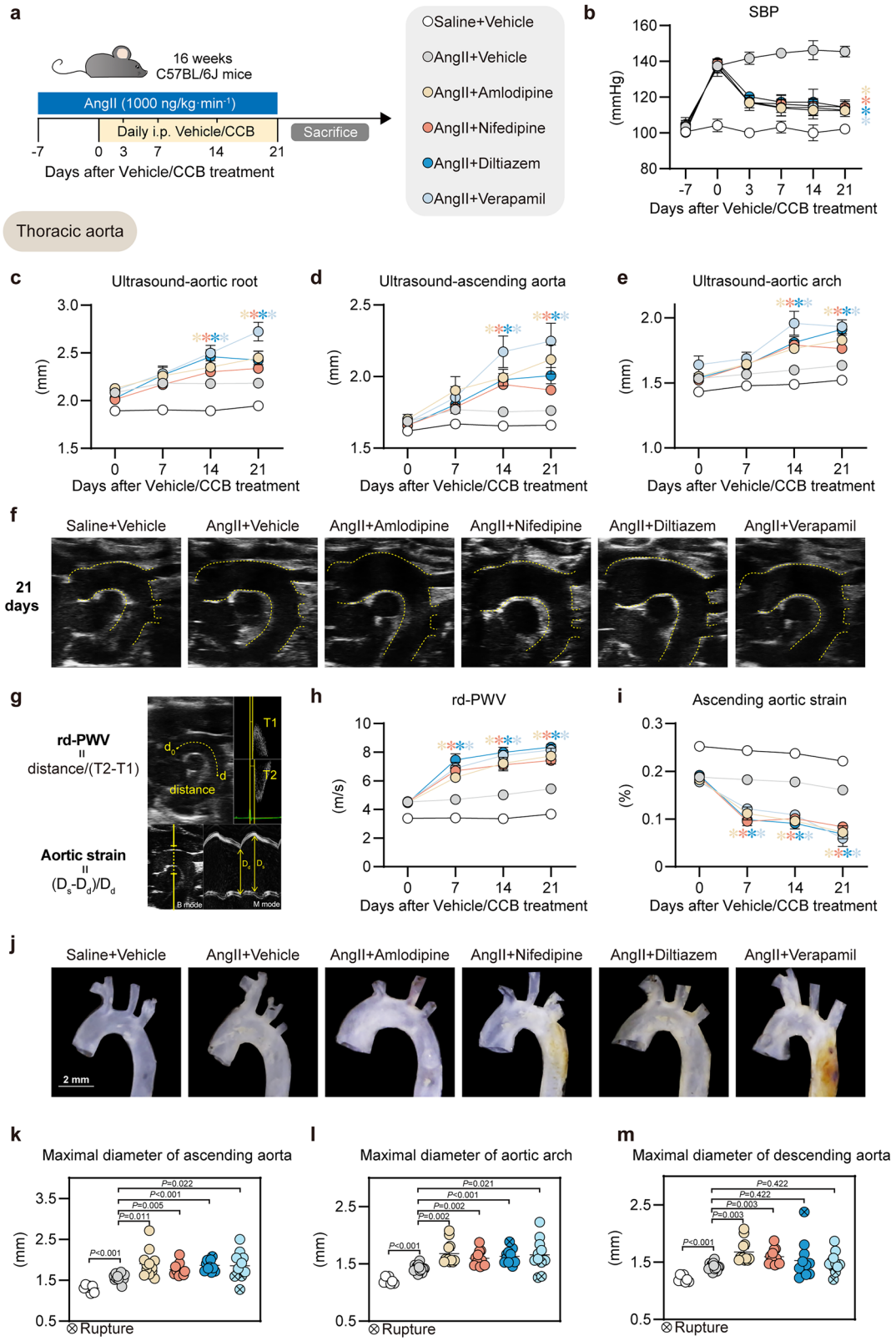

$P = 0.006$) (Fig. 2c–f). Additionally, considering the potential impact of VSMC contractility changes on vascular mechanical properties[15,19,29], we measured the thoracic root-to-descending pulse wave velocity (rd-PWV) and aortic strain in mice using M-mode ultrasound. These two indicators jointly reflect vascular stiffness and elasticity (Fig. 2g). Interestingly, compared with the AngII+Vehicle group, CCB treatment significantly increased the rd-PWV and decreased the ascending aortic strain after 7 days, with these differences becoming more pronounced after 14 and 21 days (Fig. 2h, i). These data indicate that CCB treatment increased aortic stiffness in AngII-infused mice, preceding aortic dilation. After 21 days of CCB treatment, the mice were sacrificed, and no significant differences in body weight or plasma lipid levels were observed among the groups (Supplementary Table 14). Ex vivo measurements revealed that both amlodipine and nifedipine significantly

Fig. 2 | CCBs (amlodipine, nifedipine, diltiazem, verapamil) aggravated thoracic aortic diameters in Ang II-induced aortic aneurysm mouse model. **a** Experiment design. 16-week-old C57BL/6 J mice were infused with AngII (1000 ng/kg·min^{-1}) for 28 days. After 7 days of infusion, the mice were daily injected with vehicle, dihydropyridine CCBs [amlodipine (1 mg/kg/day) or nifedipine (20 mg/kg/day)], benzothiazepine CCB [diltiazem (8 mg/kg/day)], phenylalkylamine CCBs [verapamil (12 mg/kg/day)]. **b** SBP was measured by tail-cuff at −7, 0, 3, 7, 14, 21 days after vehicle/CCBs treatment. **c**–**e** Ultrasound-monitored maximal inner diameters of the aortic root, ascending aorta, and aortic arch at 0, 7, 14, 21 days. **f** Representative ultrasound images of thoracic aorta after 21 days of vehicle/CCB treatment. **g**–**i** Monitoring of rd-PWV and ascending aortic strain in mice at different time points by M-mode ultrasound. (**g**) Schematic illustration of calculation method. (**h**) rd-PWV. **i** Ascending aortic strain. **j** Representative ex vivo morphology of thoracic aortas. Scale bar=2 mm. **k**–**m** Maximal external diameters of ascending aorta (**k**), aortic arch (**l**), and descending aorta (**m**). **Data presentation**: Data in (**b**–**e, h, i, k**-**m**) are presented as mean ± SEM. For some points, SEM is smaller than the symbol size and not visually discernible. Each data point represents an individual mouse as a biological replicate with similar results. The initial sample sizes per group were: Saline + Vehicle ($n = 7$), AngII + Vehicle ($n = 13$), AngII + Amlodipine ($n = 12$), AngII + Nifedipine ($n = 12$), AngII + Diltiazem ($n = 11$), AngII + Verapamil ($n = 11$). Due to mortality during the experimental period, exact n at each time point is provided in the Source Data file. **Statistical analysis**: Two-sided one-way ANOVA with Dunnett multiple comparisons test, Brown-Forsythe and Welch ANOVA with Dunnett T3 multiple comparisons test or Kruskal-Wallis test with Dunn's multiple comparisons was used as appropriate for (**b**-**e**, **h**, **i**) at different time points (detailed for each comparison in the Source Data file). *$P < 0.05$ vs. AngII + Vehicle group. Exact *P*-values for all comparisons are provided in the Source Data file. Statistical analysis of (**k**–**m**) were performed using two-sided Brown-Forsythe and Welch ANOVA with Dunnett T3 multiple comparisons test. Source data are provided as a Source Data file. AngII angiotensin II, SBP systolic blood pressure, CCB calcium channel blocker, rd-PWV root to descending aorta pulse wave velocity.

increased the maximum diameter of the descending aorta compared with that in AngII+Vehicle group. While the AngII+diltiazem and AngII +verapamil groups tended toward larger aortic root diameters, but this difference did not reach statistical significance compared with AngII +Vehicle group. All four CCBs significantly increased the diameters of the ascending aorta and aortic arch (Fig. 2j–m). Further Elastic Van Gieson (EVG) staining revealed that CCBs significantly exacerbated elastic fiber breakage and degradation in thoracic aortas (Supplementary Fig. 1b). Taken together, these results suggested that all types of CCBs exacerbated TAA (thoracic aortic aneurysm) expansion in AngII-infused mice. Meanwhile, ultrasound monitoring revealed a decrease in abdominal aortic strain as early as 7 days after CCB treatment, indicating increased vascular stiffness compared to the AngII +Vehicle group (Fig. 3a, b). After 14 days of CCB treatment, significant diameter expansion was observed in the suprarenal abdominal aorta, with the AngII+verapamil group showing the largest diameter (Fig. 3c). Finally, CCB treatment not only increased the maximum abdominal aortic diameter and the incidence of AAA (AngII+Vehicle, 0% [0/13]; AngII+amlodipine, 41.7% [5/12]; AngII+nifedipine, 41.7% [5/12]; AngII +diltiazem, 45.5% [5/11]; AngII+verapamil, 63.6% [7/11]) (Fig. 3d–f), but also consistently exacerbated elastic fiber degradation in the abdominal aorta (Supplementary Fig. 1c). Moreover, in an elastase-induced infrarenal AAA model, compared with the Elastase+Vehicle group, CCB treatment further increased the maximum aortic diameter and exacerbated elastic fiber degradation with no significant differences in SBP or body weight among the groups (Fig. 4a–f and Supplementary Table 15). Previous study revealed that CCBs increased ERK1/2 signal activation to accelerate aorta expansion in Marfan Syndrome[27]. Here, we observed that in AngII-pretreated VSMCs, amlodipine and verapamil significantly increased the expression of inflammatory factors (IL-6 and MCP-1) while activating ERK1/2 signal. Furthermore, treatment with the ERK1/2 inhibitor U0126 significantly blocked the CCB-induced upregulation of inflammation (Supplementary Fig. 1d, e). Taken together, these data revealed that CCBs promote the progression of both TAA and AAA.

Losartan does not attenuate thoracic and abdominal aortic aneurysm formation in AngII-infused mouse models

Next, another class of antihypertensive drugs, angiotensin II type 1 receptor blockers (ARBs), on the development of AAD was evaluated in the AngII-perfused mice model. To maintain an appropriate observation window, 24-week-old male C57BL/6 J mice were used. First, these mice were infused with AngII (1000 ng/kg/min) to induce hypertension. Seven days later, mice that died from aneurysm rupture or were confirmed to have aneurysms by ultrasound were excluded from the study. The remaining hypertensive mice received intraperitoneal losartan (10 mg/kg/day) for 21 consecutive days (Supplementary Fig. 2a and Supplementary Table 16). As shown in Supplementary Fig. 2b, AngII-induced hypertension was significantly reduced within 7 days of losartan administration. At the end of the experiment, there were no significant differences between the two groups in terms of maximum diameter of ascending aorta (2.04 ± 0.10 *vs.* 2.02 ± 0.12 mm), aortic arch (1.76 ± 0.06 *vs.* 1.67 ± 0.07 mm) and descending aorta (1.70 ± 0.06 *vs.* 1.56 ± 0.06 mm) (Supplementary Fig. 2c–f). For abdominal aorta, no significant differences were observed between AngII+Vehicle and AngII+Losartan group in terms of the AAA incidence (AngII+Vehicle, 50% [5/10]; AngII+Losartan, 60% [6/10]) or maximum diameter of abdominal aorta (1.78 ± 0.18 *vs.* 1.73 ± 0.19 mm) (Supplementary Fig. 2g-i). These results suggest that losartan may not influence the incidence or progression of aortic aneurysm in hypertensive mice.

CCBs aggravated BAPN-induced TAAD in mice

Next, we applied a BAPN-induced mouse model of TAAD. Three-week-old C57BL/6 J male mice were administered freshly prepared BAPN solution in the drinking water at a dosage of 0.5 g/kg per day for 28 days. After 7 days of BAPN treatment, the mice were injected daily with either vehicle or one of four CCBs. The control mice received normal drinking water (Fig. 5a). There were no observable differences in body weight and water intake among the BAPN groups (Supplementary Table 17). As a result, BAPN treatment led to rupture and premature death in 13.3% of the mice. Amlodipine, nifedipine, and verapamil increased the rupture and death rates, whereas diltiazem did not significantly affect mortality (Fig. 5b). Compared with the BAPN + Vehicle group, all four CCBs significantly increased the incidence of TAAD (BAPN+Vehicle, 46.7% [7/15]; BAPN+amlodipine, 100% [10/10]; BAPN+nifedipine, 100% [7/7]; BAPN+diltiazem, 85.7% [6/7]; BAPN +verapamil, 90% [9/10]) (Fig. 5c, d). Ex vivo measurements revealed significant expansion of the ascending aorta, aortic arch, and descending aorta in all CCB-treated groups compared with that in BAPN +Vehicle group (Supplementary Fig. 3a–c). EVG staining further revealed that CCBs markedly exacerbated elastic fiber breakage and degradation (Fig. 5e and Supplementary Fig. 3d). In a parallel experiment, early changes in thoracic aortic mechanical properties were detected using ultrasound (Supplementary Fig. 3e), which revealed a significant increase in rd-PWV and decrease in ascending aortic strain after as early as 3 days after the start of amlodipine and verapamil treatment. These effects occurred before any observable aortic dilation and intensified after 7 days (Fig. 5f, g and Supplementary Fig. 3f–j). Thus, CCBs aggravated BAPN-induced TAAD and aortic stiffness in mice.

CCBs application limited aortic regression in patients with Type B Aortic dissection patients following endovascular therapy

Enabled by the GUEST study (NCT04765605), a single-arm, prospective, multicenter clinical trial that primarily evaluated the

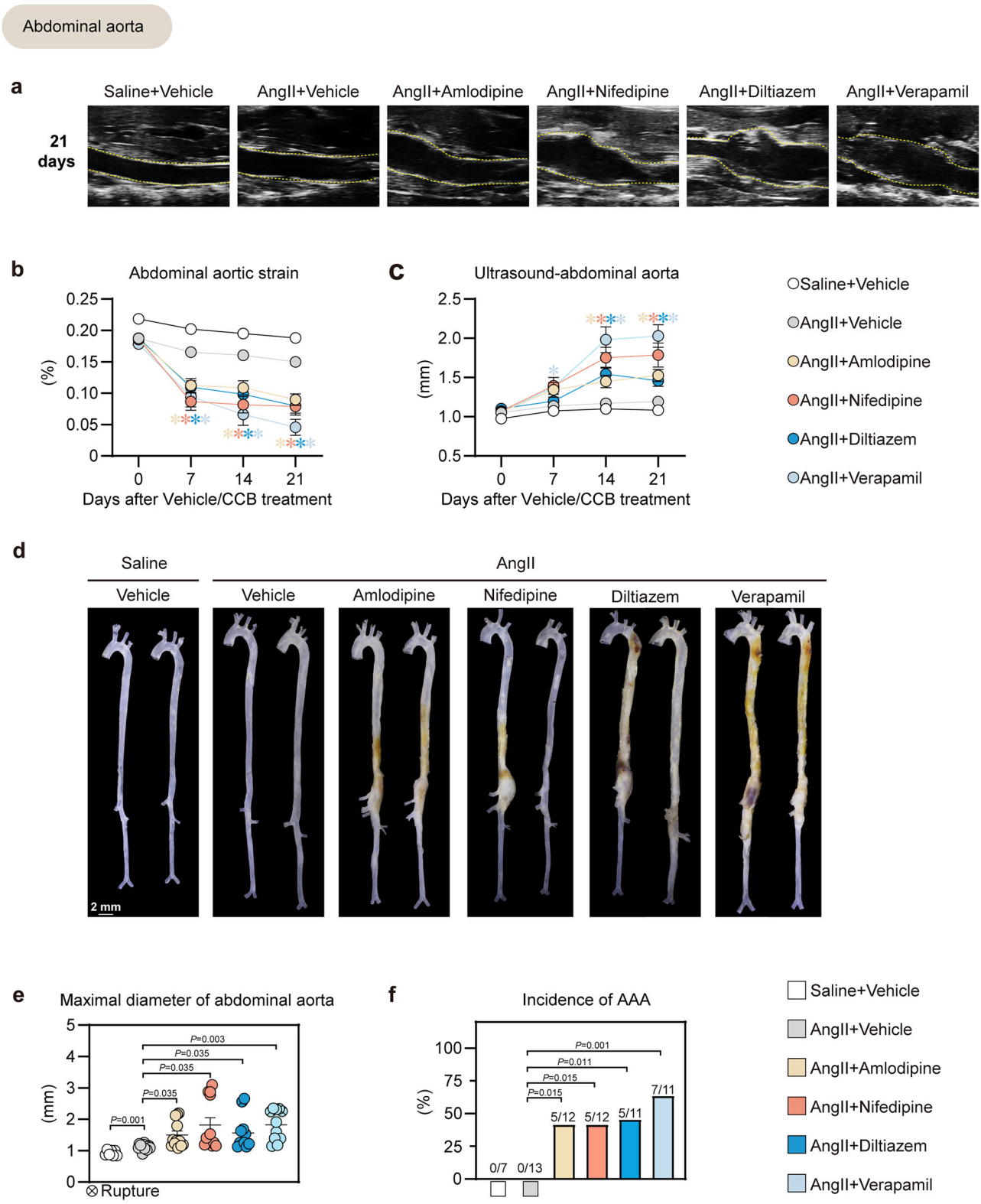

treatment efficacy of a novel stent graft system for type B aortic dissection (TBAD) (Fig. 6a), we further conducted a secondary analysis to assess the impact of CCB use on aortic expansion. In accordance with the study design, participants underwent computed tomography angiography (CTA) at 1 month, 6 months, and annually after thoracic endovascular aortic repair (TEVAR). Among the 120 enrolled participants, 95 were included in the final analysis, with 69 using CCBs, either exclusively or in combination with other antihypertensive medications and 26 using other antihypertensive medication (Fig. 6b and Supplementary Table 18). Baseline characteristics, preoperative laboratory results, and initial aortic morphology are shown in Supplementary Tables 19, 20. The alterations in aortic diameters, including those in Ishimaru zone 3 and zone 4, and the maximum descending thoracic aorta diameter (DTA max), as well as volumes in zones 3-4, zone 5, and zones 3-5, were measured and analyzed in strict accordance with the established reporting standards[30] (Fig. 6c and Supplementary Fig. 4a).

Fig. 3 | CCBs (amlodipine, nifedipine, diltiazem, verapamil) increased abdominal aortic aneurysm formation in Ang II-induced aortic aneurysm mouse model. a Representative ultrasound images of abdominal aorta after 21 days of vehicle/CCB treatment. **b**, **c** Ultrasound-monitored abdominal aortic strain (**b**), and maximal inner diameters of abdominal aorta (**c**) at 0, 7, 14, 21 days. **d** Representative ex vivo morphology of aortas. Scale bar=2 mm. **e**, **f** Maximal external diameter of abdominal aorta (**e**), and incidence of AAA (**f**). Data presentation: Data in (**b**, **c**, **e**) are presented as mean ± SEM. For some points, SEM is smaller than the symbol size and not visually discernible. Data in (**f**) are presented as as percentage (%). Each data point represents an individual mouse as a biological replicate with similar results. The initial sample sizes per group were: Saline + Vehicle ($n = 7$), AngII + Vehicle ($n = 13$), AngII + Amlodipine ($n = 12$), AngII + Nifedipine ($n = 12$), AngII + Diltiazem ($n = 11$), AngII + Verapamil ($n = 11$). Due to mortality during the experimental period, exact n at each time point is provided in the Source Data file. Statistical analysis: Two-sided Brown-Forsythe and Welch ANOVA with Dunnett T3 multiple comparisons test was used for (**b**, **c**) at different time points (detailed for each comparison in the Source Data file). $^*P < 0.05$ vs. AngII + Vehicle group for (**b**, **c**). Exact *P*-values for all comparisons are provided in the Source Data file. Statistical analysis of (**e**) were performed using two-sided Brown-Forsythe and Welch ANOVA with Dunnett T3 multiple comparisons test. Statistical analysis of (**f**) were performed using two-sided Fisher's exact test. Source data are provided as a Source Data file. CCB calcium channel blocker, AngII angiotensin II, AAA abdominal aortic aneurysm.

As a result, at the 1-year follow-up, the growth rates (%) for all indicators—including zone 3, zone 4, and DTA max diameters, as well as zones 3-4, zone 5, and zones 3-5 volumes—were significantly higher in CCB users compared to those on other antihypertensive medication. By the 2-year follow-up, these elevated growth rates remained significant for all indicators except for the zone 3 diameter (Fig. 6d). Using mixed-effects models, we observed that CCB users had greater increases in DTA max zone 4, and zone 3 diameters, as well as larger zones 3-5, zone 5, and zones 3-4 volumes, compared with those in patients using other antihypertensive medications ($P < 0.05$ for all, Supplementary Fig. 4b–g). After further adjustment for variables such as the aortic dissection phase, false lumen extension, thrombus status in the false lumen, intimal tear number and size, and initial aortic diameter and volume, differences in diameter between the two groups remained significant (zone 4: $P = 0.028$, DTA max: $P = 0.002$) and became more pronounced over time. Similarly, the adjusted differences in zones 3-4 ($P = 0.036$), zone 5 ($P = 0.006$), and zones 3-5 ($P = 0.005$) volumes were also significant and increased throughout the 2-year period (Fig. 6e, f). These findings suggest that TBAD patients who undergo TEVAR and subsequently use CCBs may experience worsened aortic regression/shrinkage.

PRKG1 silencing alleviates CCB-induced exacerbation of AAD in mice

VSMC contractility is driven primarily by the phosphorylation of the myosin regulatory light chain (p-MLC), which is positively regulated by the intracellular Ca^{2+}/calmodulin-myosin light chain kinase (MLCK) pathway. In contrast, cGMP-dependent protein kinase type I (PRKG1) enhances the activity of myosin light chain phosphatase (MLCP) by inhibiting myosin phosphatase target subunit 1 (MYPT1) phosphorylation, thereby counteracting the phosphorylation of MLC (Fig. 7a)[18,31]. Notably, a gain-of-function mutation in PRKG1 has been associated with spontaneous AAD in both patients and transgenic mice[32,33]. We did observe a significant decrease in p-MLC and p-MYPT1 levels in the aortas of verapamil-treated mice, in both AngII-induced and BAPN-induced AAD models (Fig. 7b, c). Therefore, we hypothesized that genetically inhibiting the *Prkg1* to restore VSMC contractility may mitigate CCB-induced aggravation of AAD.

An adeno-associated virus 9 (AAV9) vector containing *SM22α* promoter was designed to specifically knockdown *Prkg1* in VSMCs (Fig. 7d). Sixteen-week-old C57BL/6 J mice were intravenously injected with either AAV9-Sh_{Prkg1} or AAV9-$Sh_{Scramble}$. After 7 days, the mice received subcutaneous infusions of AngII for 28 days, followed by daily intraperitoneal injections of either vehicle or verapamil starting 7 days after AngII treatment (Fig. 7e). Ultrasound results revealed that verapamil significantly increased aortic stiffness in AAV9-$Sh_{Scramble}$-treated mice, but the differences were not observed in the AAV9-Sh_{Prkg1}-treated mice (Fig. 7f–h). As expected, in AAV9-$Sh_{Scramble}$-treated mice, verapamil significantly increased the maximum diameter of the thoracic aorta (including the aortic root, ascending aorta, and aortic arch) (Fig. 7i–l), the incidence of AAA (Fig. 7m, n), the maximum diameter of the abdominal aorta (Fig. 7o) and elastic fiber degradation (Supplementary Fig. 5a–d) compared with those associated with vehicle treatment. However, these differences were no longer present in the AAV9-Sh_{Prkg1}-treated mice. Similarly, in AAV9-Sh_{Prkg1}-or AAV9-$Sh_{Scramble}$-treated mice subjected to BAPN treatment, verapamil significantly increased the incidence of TAAD in the AAV9-$Sh_{Scramble}$ group ($Sh_{Scramble}$+Vehicle: 45% [9/20]; $Sh_{Scramble}$+Verapamil: 81.25% [13/16]), whereas *Prkg1* knockdown abolished these effects (Sh_{Prkg1}+Vehicle: 50% [5/10]; Sh_{Prkg1}+Verapamil: 40% [4/10]) (Supplementary Fig. 6a–c). Additionally, ex vivo measurements (Supplementary Fig. 6d–f) and EVG staining (Supplementary Fig. 6g, h) revealed that *Prkg1* knockdown mitigated CCB-induced aortic expansion and elastic fiber degradation, respectively. Detailed characteristics of these mice are summarized in Supplementary Tables 21, 22. Taken together, these data indicate that inhibiting the PRKG1-MLCP pathway to restore VSMC contractility can mitigate CCB-aggravated AAD formation.

Discussion

Antihypertensive drugs are commonly prescribed for AAD due to the established link between hypertension and AAD[13,14]. However, previous studies have primarily focused on the clinical use of antihypertensive drugs in patients with established AAD, while no prior studies have specifically addressed the impact of antihypertensive drugs on AAD incidence among hypertensive patients. Although impaired smooth muscle cell contractility is a known factor in AAD, whether CCBs, which inhibit smooth muscle contraction, increase AAD risk remains unclear. Herein, based on the prospective analysis of 501,878 initially AAD-free participants and 95 TBAD patients who underwent TEVAR, and AAD mouse model, we present an alarming observation that CCBs may increase the risk of AAD and the severity of post-surgical prognosis (Fig. 8).

For antihypertensives treatment in AAD, there are many different types and stages of AAD: (1) the pre-AAD stage (hypertension without AAD); (2) the diagnosed AAD stage, and (3) the post-surgical stage following AAD repair. Since patients already diagnosed with AAD are more amenable to intervention and provide a favorable window for follow-up, this stage has the most abundant RCT studies, particularly in thoracic aortic aneurysm (TAA) represented by Marfan syndrome[34–39] and small AAA[5,7]. According to current evidence, the guidelines[40,41] provided two key recommendations: (1) β-blocker or ARBs is recommended for Marfan syndrome to reduce the rate of aortic root dilatation[34,35,42]; (2) β-blocker is recommended for acute aortic dissection patients to reduce blood pressure and heart rate, thereby preventing further dissection. Apart from these recommendations, there are no RCT evaluating the effects of antihypertensive medication on non-genetic forms of TAAD and no evidence supporting their role in slowing the progression of AAA[5,7]. Of note, no studies have evaluated whether the use of antihypertensive medications influences the risk of AAD incidence in hypertensive patients. The reason for this gap may be the relatively low incidence of AAD, which requires a very large cohort size for relevant studies. Herein, by analyzing data from 501,878 initially AAD-free participants from the UKB, we found that CCB use in individuals with hypertension was associated with a significantly

https://doi.org/10.1038/s41467-025-68086-5

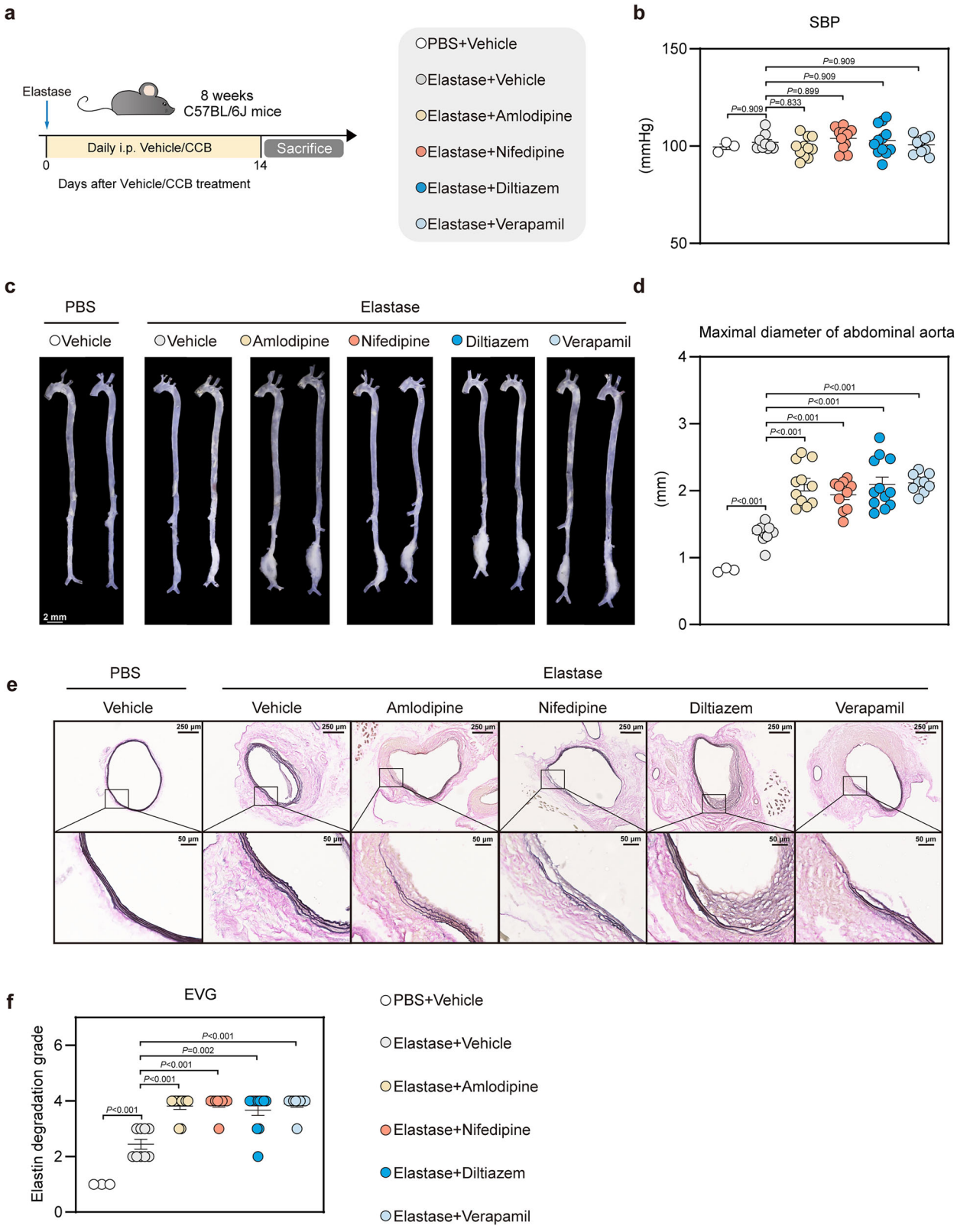

increased risk of new-onset AAD, with phenylalkylamine CCBs showing the highest risk. The main advantage of UKB analysis lies in its use of large-scale population data, overcoming the challenge of conducting RCT for AAD. Additionally, this analysis leveraged a prospective design from the UKB. These elements enabled a detailed assessment of the association between CCB use and AAD, with adjustments for potential confounders. The concurrent use of other antihypertensives was also considered to minimize indication bias, supporting the observed positive association between CCB use and AAD. Of note, non-dihydropyridine CCBs seem to exert a stronger effect on AAD, which may result from differences in their binding site on L-type calcium channels, as well as variations in pharmacokinetics and tissue selectivity, compared with dihydropyridine CCB[43–45]. Alternatively, this could result from underrepresentation of non-dihydropyridine CCB

Fig. 4 | CCBs (amlodipine, nifedipine, diltiazem, verapamil) exacerbated elastase-induced AAA and elastin degradation in mice. a Experiment design. 8-week-old mice infrarenal abdominal aortas were incubated with PBS or elastase (10 mg/ml) and then daily injected with vehicle, amlodipine (1 mg/kg/day), nifedipine (20 mg/kg/day), diltiazem (8 mg/kg/day) or verapamil (12 mg/kg/day) for 14 days. **b** SBP was measured by tail-cuff at 14 days after vehicle/CCBs treatment. **c** Representative ex vivo morphology of aortas. Scale bar=2 mm. **d** Maximal external diameter of abdominal aorta. **e**, **f** Representative image of abdominal aorta elastin Van Gieson staining (**e**) and statistical analysis on elastin degradation grade. Scale bar=250/50 μm. Data presentation: Data in (**b**, **d**, **e**, **f**) are presented as mean ± SEM. Each data point represents an individual mouse as a biological replicate with similar results. The sample sizes per group were: PBS + vehicle ($n = 3$), Elastase + vehicle ($n = 9$), Elastase + amlodipine ($n = 11$), Elastase + nifedipine ($n = 10$), Elastase + diltiazem ($n = 12$), Elastase + verapamil ($n = 9$). Statistical analysis: Statistical analysis of (**b**) were performed using two-sided one-way ANOVA with Dunnett multiple comparisons test. Statistical analysis of (**d**) were performed using two-sided Brown-Forsythe and Welch ANOVA with Dunnett T3 multiple comparisons test. Statistical analysis of (**f**) were performed using two-sided Kruskal-Wallis test with Dunn's multiple comparisons. Source data are provided as a Source Data file. CCB calcium channel blocker, PBS phosphate buffered saline, SBP systolic blood pressure.

users in the cohort, reducing statistical power and introducing uncertainty. Moreover, we observed that other classes of antihypertensive drugs did not significantly affect AAD incidence—a result consistent with previous RCTs showing ACEIs and ARBs do not reduce AAA growth rates[5,7]—though these "other antihypertensive medications" may cause statistical mutual dilution of different drug effects. Of interest, several studies reported a potential protective effect of amlodipine and diltiazem against AngII-induced AAD in hyperlipidemic mice[24,25]. However, the doses used in those studies were 5-10 times higher than those in our study or clinical practice. Furthermore, previous studies exclusively applied concurrent CCBs and AngII on the establishment of the hypertension model, which led to the failure of hypertension induction[23,26]. In our study, to mimic the bona fide situation of hypertensive populations, we implanted AngII pumps in 4-month-old wild-type mice for one week to establish hypertension prior to administering CCB drugs. In a similar model, we also observed that losartan lowers blood pressure but does not affect the occurrence and progression of AAD. This finding is consistent with the results from the UKB analysis and previous studies demonstrating that losartan does not attenuate AAD induced by elastase, BAPN, or DOCA[46–48].

Another intriguing finding of the current study is that impaired VSMC contractility is a key factor in the exacerbation of AAD induced by CCBs. Previous research has linked mutations in essential contractile genes (*MYH11* and *ACTA2*)[49,50] and regulators such as *MLCK*[51] and *PRKG1*[33] to AAD formation. Additionally, several drugs that may impair VSMC contractility, such as sildenafil and fluvastatin, have been shown to aggravate aneurysm progression[52,53]. However, the exact mechanisms by which VSMC contraction dysfunction contributes to AAD remain unclear. Herein, data from a natural population cohort, a prospective post-AAD cohort, and animal models consistently demonstrated that CCB use, which inhibits VSMC contractility, significantly increased the risk of AAD. This raises the following question: why does CCB-induced inhibition of VSMC contractility worsen AAD? We found that CCB treatment in AAD model mice significantly suppressed VSMC contractility, as characterized by decreased MLC and MYPT-1 phosphorylation. In contrast, in vivo knockdown of PRKG1, which is an endogenous inhibitor of MLC phosphorylation and can directly phosphorylate the α1c subunit of the L-type calcium channel CaV1.2 (e.g., at the Ser1928 site), suppressing Ca^{2+} influx[54], restored VSMCs contractility and notably mitigated the CCB-induced exacerbation of AAD. This finding aligns with prior findings showing that gain-of-function mutations in PRKG1 lead to spontaneous aortic dissection, whereas PRKG1 knockdown or inhibition reduces aortic dilation in MFS mice and elastase-induced AAA models[53,55]. Using ultrasound, we observed that in both AngII- and BAPN-induced AAD models, CCB treatment increased rd-PWV and reduced aortic strain, indicating increased aortic stiffness and decreased elasticity. Notably, these mechanical changes occurred before aortic dilation and aneurysm formation, consistent with earlier studies showing increased aortic stiffness in AAA patients treated with CCBs and elevated VSMC stiffness in tissues from TAAD or AAA patients and animal models[19,29,56,57]. The potential mechanism by which CCBs increase aortic stiffness include directly inhibiting the contraction of VSMCs and thus impairing their ability to regulate aortic compliance[15,58], promoting the phenotypic switching of VSMCs to a synthetic phenotype to enhance collagen secretion and deposition[27,59], and inhibiting the calcium-dependent endothelial nitric oxide synthase (eNOS) activity in endothelial cells to reduce NO production[60]. Our findings underscore the critical role of VSMC contractility in AAD progression and suggest that ultrasound monitoring of vascular mechanics may serve as an effective strategy for early warning, prediction and intervention of AAD. Whether other drugs affecting contractility, such as nitrates, potassium channel openers, and Rho kinase inhibitors, may also exacerbate AAD and warrant further investigation.

Regarding the association between postoperative CCB use and outcomes in patients with AAD after surgical repair, our study found that in TBAD patients undergoing TEVAR, subsequent CCB use was associated with worsened aortic regression/shrinkage. Current guidelines do not provide specific recommendations regarding antihypertensive therapy after AAD surgery, except for suggesting long-term use of β-blockers after aortic dissection to control heart rate and blood pressure (without an assigned level of evidence)[40,41]. To date, only a dozen retrospective studies have investigated the association between antihypertensive medications and outcomes after aortic repair, but the findings remain inconsistent[61–73]. The main reason is that these studies differed substantially in patient populations, study methodologies, surgical approaches (endovascular versus open repair), operative techniques, and graft materials used. In our study, all patients had TBAD and underwent TEVAR with the same stent graft system and a standardized implantation protocol, which substantially minimized potential confounding factors. In addition, we selected postoperative aortic regression/shrinkage as the primary outcome, which is endorsed by the ESC guidelines as a key indicator of low-risk aneurysms during postoperative surveillance[41] and is associated with improved 5 - 10-year survival as well as reduced rates of secondary interventions[74,75]. It should be emphasized that this aortic regression/shrinkage does not reflect an acute alteration in vascular tone induced by antihypertensive therapy, as we observed a progressive divergence in aortic diameters and volumes over time between the CCB and non-CCB groups during the 2-year follow-up period. Therefore, this may reflect CCB-induced postoperative aortic remodeling, highlighting the importance of careful selection of antihypertensive therapy in this population and underscoring the urgent need for safer and more effective strategies for both AAD prevention and postoperative management.

In summary, our findings highlight a concerning observation, indicating the detrimental impact of CCBs on the risk of AAD.

Methods

UKB study population

The UK Biobank (UKB) is a large population-based cohort, including over 500,000 volunteers aged between 40 and 69 years across England, Scotland, and Wales recruited between 2006 and 2010 (Details could be found at https://www.ukbiobank.ac.uk). All UKB participants provided informed consent via an electronic signature at the beginning of the process and the UKB had ethical approval from the North

https://doi.org/10.1038/s41467-025-68086-5

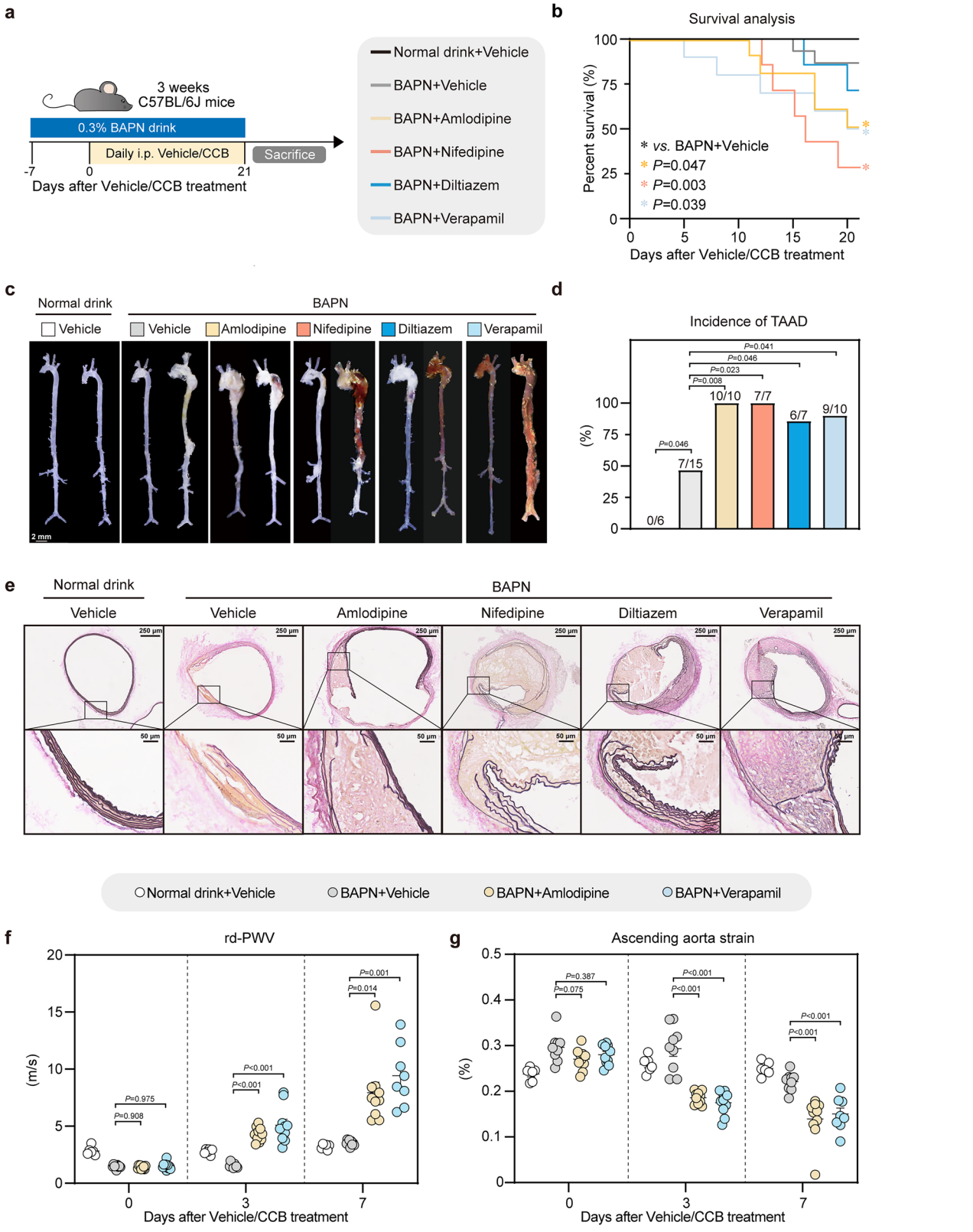

West Multi-Center Research Ethics Committee (REC ref. 16:/NW/0274). Included were 501,878 participants in this study after removing participants who withdrew from the UKB and prevalent aortic aneurysm and dissection (AAD). We also investigated the association between subtypes of CCBs and AAD in the participants with prevalent hypertension ($n = 142,419$) and the association between the CCBs use and all-cause mortality in the participants with prevalent aortic aneurysm and dissection ($n = 509$).

Assessment of exposure

Baseline hypertension was defined through self-reported hypertension during nurse interview, and self-reported questionnaires regarding

Fig. 5 | CCBs (amlodipine, nifedipine, diltiazem, verapamil) aggravated BAPN-induced TAAD in mice. a Experiment design. 3-week-old mice were treated with 0.3% BAPN in drinking water (0.5 g/kg per day) for 28 days. Normal drink served as negative control. After 7 days of BAPN treatment, mice were daily injected with vehicle or different CCBs: amlodipine (1 mg/kg/day), nifedipine (20 mg/kg/day), diltiazem (8 mg/kg/day), verapamil (12 mg/kg/day). **b** Survival analysis of mice after vehicle/CCB treatment. **c** Representative ex vivo morphology of aortas. Scale bar=2 mm. **d** Incidence of TAAD. **e** Representative image of thoracic aorta elastin Van Gieson staining. Scale bar = 250/50 μm. **f**, **g** Three-week-old mice were treated with 0.3% BAPN in drinking water (0.5 g/kg per day) for 7 days. Then, they were daily injected with vehicle, amlodipine (1 mg/kg/d) or verapamil (12 mg/kg/d) for another 7 days. Rd-PWV (**f**) and ascending aorta strain (**g**) were measured by ultrasound at different time points. Data presentation: Data in (**b**, **d**) are presented as percentage (%). Data in (**f**, **g**) are presented as the mean ± SEM. Each data point represents an individual mouse as a biological replicate with similar results. The sample sizes per group for (**a**–**e**) were normal drink + vehicle ($n = 6$), BAPN + vehicle ($n = 15$), BAPN + amlodipine ($n = 10$), BAPN + nifedipine ($n = 7$), BAPN + diltiazem ($n = 7$), BAPN + verapamil ($n = 10$). The sample sizes per group for (**f**, **g**) were: normal drink + vehicle ($n = 6$), BAPN + vehicle ($n = 9$), BAPN + amlodipine ($n = 10$), BAPN + verapamil ($n = 10$). Due to mortality during the experimental period, exact n at each time point is provided in the Source Data file. Statistical analysis: Statistical analysis of (**b**) were performed using two-sided Logrank test. $^*P < 0.05$ vs. BAPN + Vehicle group. Statistical analysis of (**d**) were performed using two-sided Fisher's exact test. Statistical analysis of (**f**, **g**) were performed using two-sided one-way ANOVA with Dunnett multiple comparisons test, Brown-Forsythe and Welch ANOVA with Dunnett T3 multiple comparisons test or Kruskal-Wallis test with Dunn's multiple comparisons at different time points (detailed for each comparison in the Source Data file). Source data are provided as a Source Data file. TAAD thoracic aortic aneurysm and dissection, CCB calcium channel blocker, Rd-PWV root to descending aorta pulse wave velocity, BAPN β-aminopropionitrile.

high blood pressure diagnosed by doctor, hospital data via international classification of diseases (ICD) codes for essential (primary) hypertension, hypertensive disease with or without heart failure, hypertensive heart and renal diseases, and secondary hypertension according to previous study[76] (Supplementary Table 1). A high concordance was observed between self-reported (either self-reported hypertension during nurse interview or self-reported high blood pressure diagnosed by doctor) and hypertension identified through hospital records, with more than 94% of individuals who self-reported hypertension also having a physician-confirmed diagnosis based on ICD codes. We also adopted a broader definition of hypertension by further incorporating antihypertensive medications use in the sensitivity analysis. Antihypertensive medications regarding calcium channel blocker use (Supplementary Table 2) and other blood pressure lowering medications including renin-angiotensin system inhibitors, beta blockers, diuretic, or multiple antihypertensive classes were assessed at baseline[76,77] (Supplementary Table 3). All self-reported medications were recorded and subsequently confirmed by a trained nurse in an interview conducted during the same visit. Additionally, participants who reported taking a blood pressure medication (via Field IDs 6153 and 6177) without using CCBs were categorized under the "other antihypertensive medications" group (excluding CCB use). Anyone reporting concurrent CCB use was categorized into the CCBs group, including those using CCBs exclusively or in combination with other antihypertensive medications. There was no recorded information concerning the dosage, frequency, or duration of use for medication. We categorized groups according to hypertension status and antihypertension medications (Fig. 1).

Assessment of covariates

At baseline, data on sociodemographic factors (age, sex, education, and ethnicity), BMI, and lifestyle factors (smoking status and alcohol use) were collected through questionnaires and verbal interviews. Total cholesterol, total triglycerides, and systolic blood pressure were also analyzed in this study, regarding to the risk of AAD. Specifically, serum lipid levels were measured by biochemical assays from the blood samples collected at baseline by Beckman Coulter AU5800 Platform. Total cholesterol and total triglycerides were analyzed using glycerol-3-phosphate (GPO)-peroxidase (POD) chromogenic method. The resting blood pressure was measured by Omron 705 IT electronic blood pressure monitor. During the blood pressure measurement, the participant was instructed to sit with their feet parallel, toes pointing forward, and the soles of both feet flat on the floor. The right arm was only used if the left was not feasible. The mean value of blood pressure readings would be calculated and used in this analysis if there were more than one measurement within a few minutes available; otherwise, electronic blood pressure monitor values were preferred, and manual readings would be used if there were no electronic blood pressure readings.

Assessment of outcome

AAD cases and its subtypes including thoracic aortic aneurysm and dissection (TAAD) and abdominal aortic aneurysm (AAA) were identified from the UKB using hospital inpatient records where these conditions were documented as either primary or secondary diagnosis, or linkage to death register data using the International Classification of Disease (ICD) coding 10 (Supplementary Table 4).

Materials

Amlodipine (HY-B0317), Nifedipine (HY-B0284), Diltiazem (HY-14656), Verapamil (HY-14275), Losartan (HY-17512), human angiotensin II (HY13948) was purchased from Med Chem Express (Monmouth Junction, NJ, USA). Osmotic pumps (2004W) were purchased from RWD Life Science Co (Shenzhen, Guangdong, China). Elastase, porcine pancreas (HY-P2974) was purchased from Med Chem Express (Monmouth Junction, NJ, USA). β-aminopropionitrile monofumarate (BAPN, A3134) was purchased from Sigma Aldrich (St. Louis, MO, USA). PEG200 (P8490), Tween 80 (T8360) and protein phosphatase inhibitor (P1260) were purchased from Solarbio (Beijing, China). Antibodies against GAPDH (10494), PRKG1 (21646) were purchased from ProteinTech (Chicago, IL, USA). Antibody against p-MLC (3671), MLC (8505), p-MYPT1 (4563), p-ERK1/2 (9101) was purchased from Cell signaling Technology (Boston, MA, USA). ERK1/2 (T40071F) was purchased from Almart (Shanghai, China).

Animals

Animal studies were conducted in compliance with the guidelines of the Institutional Animal Care and Use Committee of Peking University Health Science Center and were approved by the Biomedical Ethics Committee of Peking University. SPF mice of C57BL/6 J were purchased from the Experimental Animal Science Center and raised in the Experimental Animal Science Center of Peking University Health Science Center, Beijing, China. The mice were randomly assigned to different groups and housed in cages with 4–6 mice per cage with unrestricted access to rodent feed and water. Specifically, a light-dark cycle was established with lights on from 8 a.m. to 8 p.m., while maintaining a temperature range of 21-24 °C and humidity levels between 40–70%. Mice for surgeries were anesthetized with isoflurane (1.5%–2%). All animals were anesthetized with 1.25% avertin before being sacrificed. For plasma samples, blood was collected from the heart with heparin sodium (250 U/ml), followed by centrifugation for 10 min at 3000 rpm. For aorta protein samples, mice were perfused with ice-cold saline, and then the aorta was isolated. For aortic morphology studies, the mice were successively perfused with 10% KCl, 10×PBS, and 4% paraformaldehyde. Then, the aortas were dissected from the root to the iliac bifurcation in all animal models for further analysis.

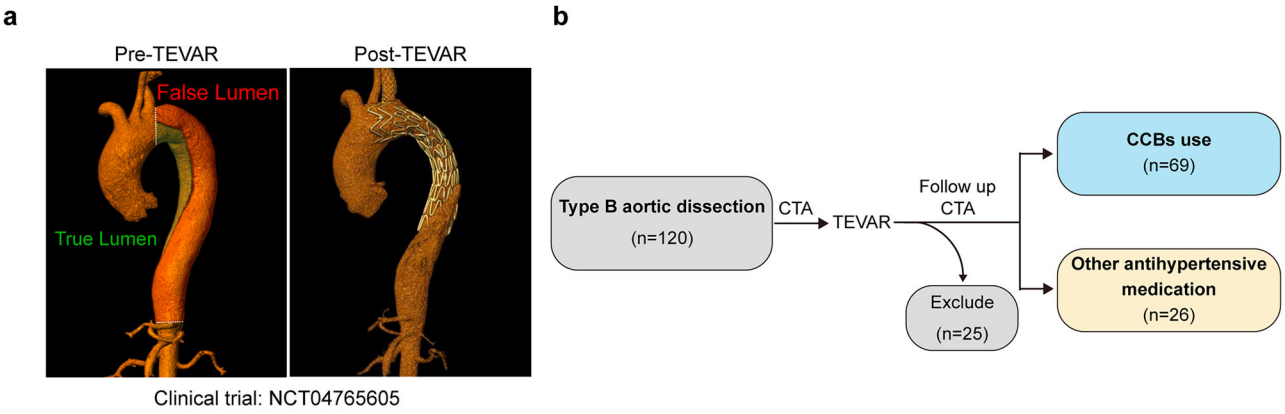

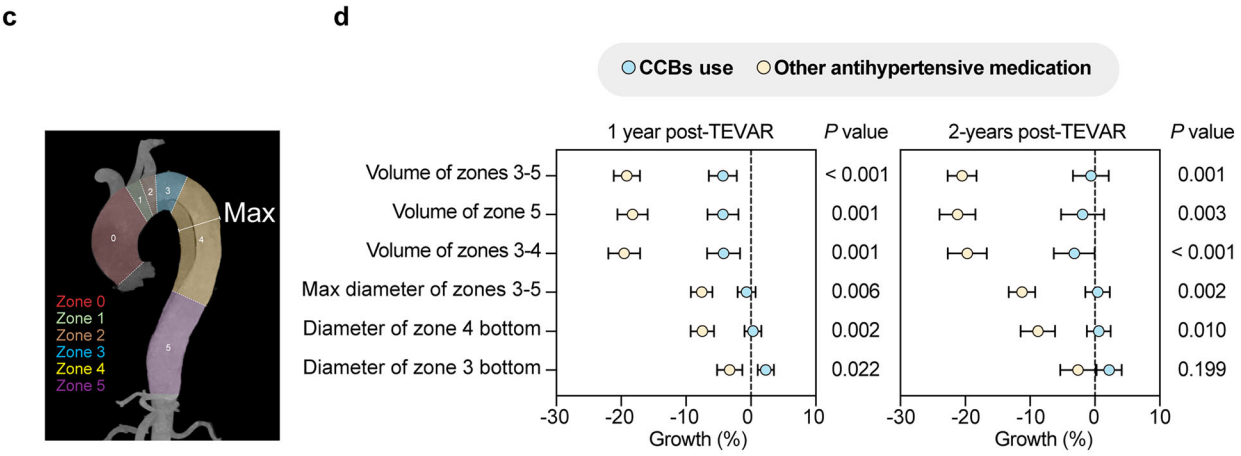

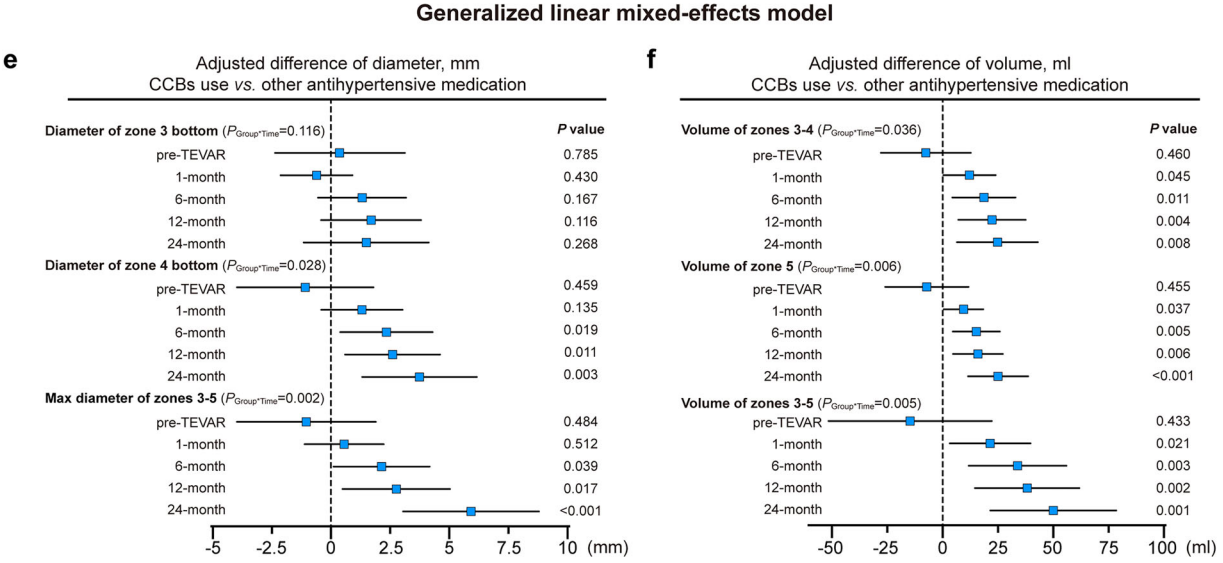

Drugs dissolution and injection

The doses of drugs used in the experiment were converted from clinical recommended human doses to mouse doses according to the FDA's guidance for dose translation (https://www.fda.gov/media/72309/download, conversion factor=12.3). The specific doses were as follows: amlodipine (1 mg/kg/day), nifedipine (20 mg/kg/day), diltiazem (8 mg/kg/day) and verapamil (12 mg/kg/day), losartan (10 mg/kg/day). The dissolution protocol used a gradient of DMSO, PEG 200, Tween 80, and saline. The final CCB injection solution consisted of 2% DMSO, 8% PEG 200, 1% Tween80, and 89% saline. Experimental mice were administered the specified dose of CCBs or vehicle daily via intraperitoneal injection based on body weight, continuing until the sacrifice endpoint.

Angiotensin II-induced aortic aneurysm mouse model

Sixteen-week-old C57BL/6 J mice were subcutaneously infused with minipumps containing AngII (1000 ng/kg·min^{-1}) for 28 days. After 7 days of AngII infusion, images of mice thoracic and abdominal aorta were obtained via ultrasound instrument. During hypertension establishment phase, (1) mice died due to aortic aneurysm rupture; or (2)

Fig. 6 | The application of CCBs limited aortic regression in patients with Type B Aortic Dissection Patients following endovascular therapy. a The representative computed tomography angiography (CTA) images of the thoracic aorta in patients with TBAD, showing the condition before (left) and after (right) the application of the covered stent graft system-Weflow-Tbranch™ (a single-embedded branch thoracic aortic covered stent graft system) for endovascular repair. **b** Patient screening flowchart. **c** The representative CTA images of a patient before TEVAR surgery show the segmentation of the aorta. Zone 3 (2 cm distal to the left subclavian artery, shown in blue), zone 4 (from the left subclavian artery to the mid - point of the descending thoracic aorta, shown in yellow), and zone 5 (from the mid - point of the DTA to the superior border of the celiac artery, shown in purple). **d** The growth rates of aortic diameter/volume of patients one and two years after TEVAR surgery. Growth rate (%) = (post-diameter/volume - pre-diameter/volume) / pre - diameter/volume. **e**, **f** Adjusted difference of aortic diameters (**e**), and volumes (**f**) at pre-TEVAR and 1, 6, 12, 24 months after TEVAR (CCBs use *vs.* other antihypertensive medication). Data presentation: Data in (**d**) are presented as the mean ± SEM. Each data point represents an individual patient as a biological replicate with similar results. The sample sizes per group were CCB use ($n = 68$), other antihypertensive medication ($n = 25$) for 1-year post-TEVAR and CCB use ($n = 44$), other antihypertensive medication ($n = 14$) for 2-year post-TEVAR. Exact n at each time point is provided in the Source Data file. Data in (**e**, **f**) are presented as: squares represented β value and error bars represented 95% CIs. Statistical analysis: Statistical analysis of (**d**) were performed using two-sided Student's T test. Statistical analysis of (**e**, **f**) were performed using two-sided generalized linear mix-effects model adjusted for age (years), sex (men; women), systolic blood pressure (mmHg), family history of cardiovascular disease (yes; no), diabetes (yes; no), hyperlipidemia (yes; no), coronary heart disease (yes; no), false lumen length grades (1–8), total false lumen thrombus score (0;1;2;3 levels for each zone and plus all zones for total score), distal tear numbers (zones 5–9), first tear diameter (mm), and time interactions with CCBs. *P*-values were present in the figure and detailed information refer to source data. Source data are provided as a Source Data file. TEVAR thoracic endovascular aortic repair. TBAD type B aortic dissection, CCB calcium channel blocker, CTA computed tomography angiography.

mice diagnosed with developed aorta aneurysm by ultrasound imaging (TAA or AAA: defined as a segmental aortic diameter > 1.5 times that of the adjacent normal aorta) were excluded from the study and those hypertensive mice without AAD were remained. Subsequently, those hypertensive mice without AAD were daily injected with vehicle or one of four CCBs: amlodipine, nifedipine, diltiazem or verapamil (Supplementary Fig. 1a). SBP was recorded at 0, 3, 7, 14, 21 days after vehicle/CCBs treatment. Root-descending aorta pulse wave velocity, ascending and abdominal aorta strain, thoracic and abdominal aorta diameters were detected at 0, 7, 14, 21 days after vehicle/CCBs treatment by ultrasound. For losartan experiment, six month-old C57BL/6 J mice were infused with AngII (1000 ng/kg·min^{-1}) for 28 days. After 7 days of infusion, the mice were daily injected with vehicle or losartan (10 mg/kg/day). SBP was recorded at 0, 7, 14, 21 days after vehicle/losartan treatment.

At the sacrificed endpoint, aortas were dissected for ex vivo measurements of the maximal thoracic aorta diameter (ascending aorta, aortic arch, descending aorta) and abdominal aorta diameter. Aortic aneurysm was evaluated in the suprarenal abdominal aorta (referred to as AAA) and the aortic root and ascending aorta (referred to as TAA). The maximal diameters of the root, ascending and suprarenal aortas were calculated by statistical analysis, and the aortic aneurysm was defined as an aorta with a diameter more than 1.5 times larger than its adjacent normal aorta.

Elastase-induced abdominal aorta aneurysm mouse model

Eight-week-old C57BL/6 mice were used for surgery. Briefly, the mice were anesthetized and the infrarenal aortas were exposed, isolated, and wrapped with sterile cotton, which was soaked with 25 µl of elastase (10 mg/ml) for 40 min. PBS was used as negative control. Then, the elastase-soaked cotton was removed, and 0.9% NaCl was used to perfuse the abdominal cavity before suturing. Subsequently, these mice were administered intraperitoneal injections of vehicle or four CCBs for 14 days.

At sacrificed endpoint, systolic blood pressures were measured and aortas were dissected for ex vivo measurements of the maximal abdominal aorta diameter.

BAPN-induced TAAD mouse model

Three-week-old C57BL/6 mice were treated with 0.3% BAPN in drinking water (0.5 g/kg per day) for 28 days. The drinking water was refreshed every 3 days. Normal drinking was designed as negative control. After 1 week, the mice were daily injected with vehicle or four CCBs. It is important to note that due to the small size of the TAAD model mice and the potential risk of TAAD rupture induced by stress during blood pressure measurement, this model is not suitable for recording SBP.

At the sacrificed endpoint, aortas were dissected for ex vivo measurements of the maximal thoracic aorta diameter (ascending aorta, aortic arch and descending aorta). The incidence rate of TAAD and related mortality were recorded. TAAD was defined as thoracic aortic dissection (aortic false lumen formation) and/or thoracic aortic aneurysm (at least 1.5 times extension of aortic diameter). Overall, any of the following criteria was defined as TAAD: 1. The deceased mice displayed blood clotting in the thoracic cavity. 2. EVG staining revealed aortic false lumen formation. 3. > 1.5 times extension of aortic diameter compare to negative control.

In another parallel BAPN experiment, ultrasound was used to measure root-descending aorta pulse wave velocity, ascending aorta strain, thoracic aorta diameters at 0, 3, 7 days after vehicle/amlodipine/verapamil treatment.

Mouse blood pressure measurement

Mouse blood pressure was measured according to the previous study[78]. Briefly, a noninvasive computerized CODA tail-cuff blood pressure system (Kent Scientific, Torrington, CT, USA) was used to measure mouse SBP. The equipment was maintained in a clean state, free from foreign scents or blood odors. The investigator was blinded to the experimental groups when performing the measurements, and the mice were tested in a randomized order. All mice underwent training sessions from 1 to 4 PM on 7 consecutive days to become accustomed to the tail-cuff procedure.

Mouse aortic ultrasound

Vevo LAZR system (FUJIFILM VisualSonics, Canada) was used to measure aorta parameters in mice, including thoracic aortic diameter, abdominal aortic diameter, root to descending pulse wave velocity (rd-PWV), ascending aorta and abdominal aorta circumferential strain. Mice were anaesthetized by 1.5–2% isoflurane and placed on the platform that carries electrocardiogram (ECG) electrodes. Conductive gel was applied to the electrodes on the animal platform, and the mouse's paws were secured onto the electrode pads with tape to ensure accurate ECG acquisition. The mouse's body temperature and respiratory rate were maintained, with the heart rate kept within the range of 400–550 bpm during the acquisition. MX transducer MX550D (centre transmit: 40 MHz; axial resolution: 40 µm) was used. The thoracic and abdominal aorta diameters were recorded by B-mode ultrasonography. For aorta diameter, images of the aortic arch cross-section (the operation table was tilted 15° to the right, and the probe arm was tilted 30-45° to the left) and abdominal aorta sagittal section (the probe was positioned perpendicular to the animal) were obtained. Rd-PWV was measured using ultrasound imaging by B-mode and Doppler-Mode. The vascular pulse-wave

https://doi.org/10.1038/s41467-025-68086-5

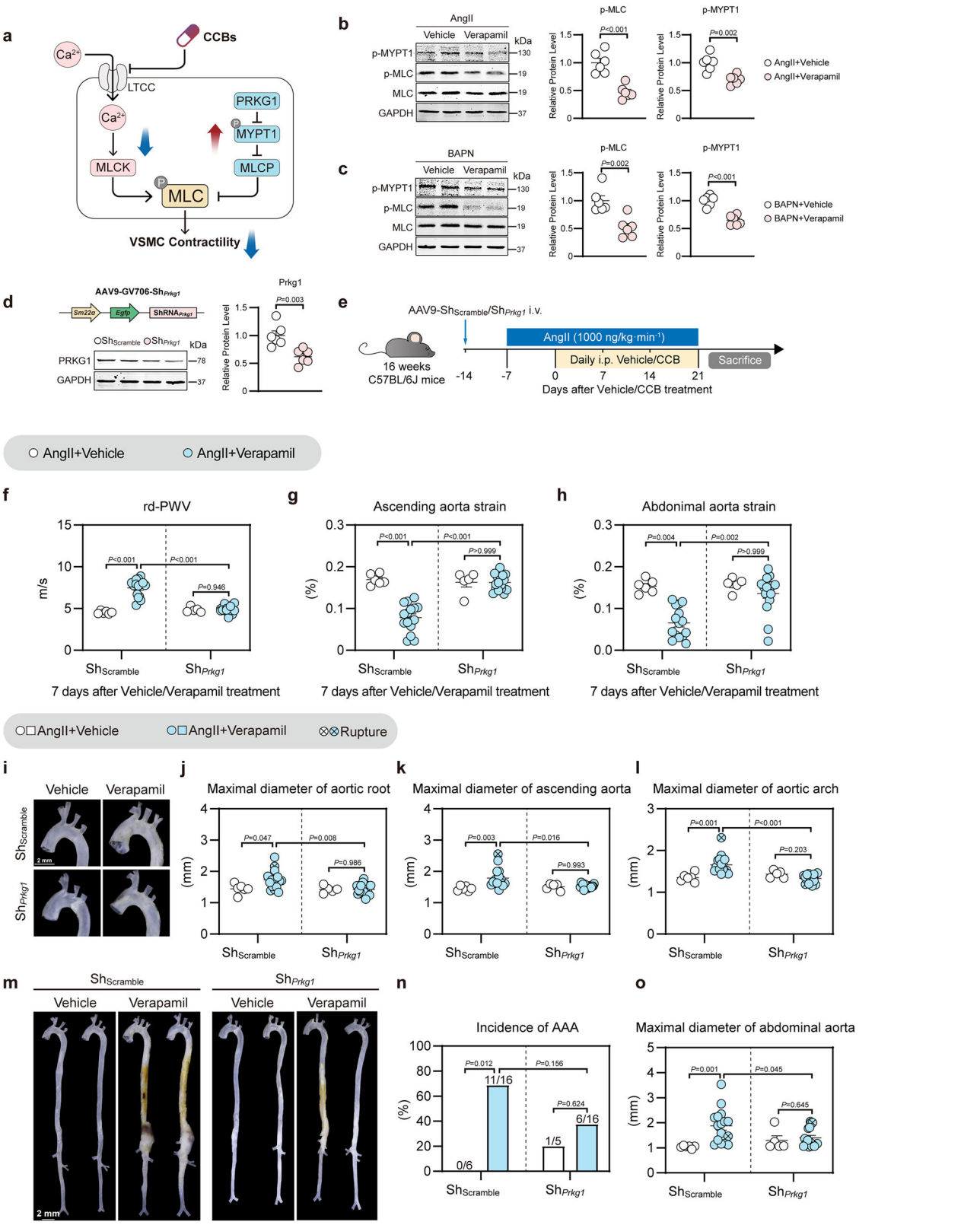

Doppler tracing was recorded at the position of root (position 1, d0). The time from the R point of QRS to the onset of the Doppler waveform was measured (T1). Then another position in the descending aorta was selected and the pulse-wave Doppler tracing was recoded (position 2, d). The time from the R point of QRS to the onset of the Doppler waveform was measured (T2). The distance between position 1 and position 2 was measured (distance). Rd-PWV is calculated as: distance/(T2−T1) (m/s). The values for T1 and T2 were the average of three to five measurements. For ascending aorta and abdominal aorta circumferential strain, the systolic diameter (Ds) and diastolic diameter (Dd) were measured, and circumferential cyclic strain was calculated as (Ds-Dd)/Dd. The values for Ds and Dd were the average of three to five measurements.

Fig. 7 | Silencing of *Prkg1* mitigates CCB-aggravated AAD in mice. a Diagram of the signaling involved in vascular smooth muscle cell contraction. **b**, **c** Representative western blot image and statistical analysis of MLC phosphorylation, and MYPT1 phosphorylation in aortas from (**b**) mice infused with AngII (1000 ng/kg·min^{-1}) for 7 days or (**c**) treated with 0.3% BAPN for 3 days followed by injection of vehicle or verapamil (20 mg/kg/d) for 1 hour. **d** Illustration of the AAV9 vector and statistical analysis of PRKG1 protein level in aorta from mice treated with AAV9-Sh$_{Prkg1}$ for 2 weeks. **e** 16-week-old C57BL/6 J mice were intravenously injected with AAV9-Sh$_{Prkg1}$ or AAV9-Sh$_{Scramble}$ for 1 weeks. Then, mice were infused with AngII (1000 ng/kg·min^{-1}) for 28 days. After 7 days of AngII infusion, the mice were daily injected with vehicle/verapamil (12 mg/kg/day). **f**–**h** Ultrasound-monitored rd-PWV (**f**), ascending aorta strain (**g**), and abdominal aorta strain (**h**) at 7 days after vehicle/verapamil treatment. **i**–**o** Representative ex vivo morphology of thoracic aortas (**i**). Scale bar=2 mm. Maximal diameters of aortic root (**j**). Maximal diameters of ascending aorta (**k**). Maximal diameters of aortic arch (**l**). Representative ex vivo morphology of aortas (**m**). Scale bar=2 mm. Incidence of AAA (**n**). Maximal diameters of abdominal aorta (**o**). Data presentation: Data in (**b**–**d, f**–**h, j**–**l, o**) are presented as the mean ± SEM. Data in (**n**) are presented as percentage (%). Each data point represents an individual mouse as a biological replicate with similar results. The sample sizes per group for (**b**-**d**) were $n = 6$. The sample sizes per group for (**f**–**o**) were Sh$_{Scramble}$ + AngII + vehicle ($n = 6$), Sh$_{Scramble}$ + AngII + verapamil ($n = 16$); Sh$_{Prkg1}$ + AngII + vehicle ($n = 5$); Sh$_{Prkg1}$ + AngII + verapamil ($n = 16$). Exact n is provided in the Source Data file. Statistical analysis: Statistical analysis of (**b**–**d**) were performed using two-sided Student's T test. Statistical analysis of (**f**, **g, j**–**l**, **o**) were performed using two-sided Brown-Forsythe and Welch ANOVA tests with Games-Howell multiple comparisons. Statistical analysis of (**h**) were performed using Kruskal-Wallis test with Dunn's multiple comparisons. Statistical analysis of (**n**) were performed using two-sided Fisher's exact test. Source data are provided as a Source Data file. LTCC L-type calcium channel, MLC myosin regulatory light chain, MLCK myosin light chain kinase, PRKG1 protein kinase G type 1, MLCP myosin light chain phosphatase, MYPT1 myosin phosphatase target subunit 1, AAA abdominal aortic aneurysm, TAAD thoracic aortic aneurysm and dissection, Rd-PWV root-descending pulse wave velocity.

Blood biochemical analysis

Blood samples were collected and underwent centrifugation. The quantification of plasma cholesterol and triglyceride levels was performed using commercially available kits (#100000220, Zhong Sheng Biotechnology).

Elastin *Van Gieson* staining

Cryosections of the lesion aorta (8 μm thick) were analyzed by elastic *Van Gieson* staining (BASO Precision Optics Ltd., Taiwan, China) according to the manufacturer's protocol for elastin assessment. Elastin degradation graded as grade 1, <25% degradation; grade 2, 26% to 50% degradation; grade 3, 51% to 75% degradation; grade 4, > 75% degradation.

Adeno-associated virus 9 (AAV9) production and infection

A plasmid (GV706) encoding promoter *SM22α*, *EGFP* and shRNA targeting mouse *Prkg1* was engineered by cloning the following shRNA into the AAV9 vector:

Sh$_{Prkg1}$ (sense) 5′-GATCCCCGGAGAATCTCATCCTAGATCTCGAGATCTAGGATGAGATTCTCCGGTTTTTGC-3′;

Sh$_{Prkg1}$(antisense) 5′-GGCCGCAAAAACCGGAGAATCTCATCCTAGATCTCGGATCTAGGATGAGATTCTCCGGG-3′;

The sequence of the mouse *Prkg1* shRNA was referred to the previous study[55]. Packaging and producing work were performed by GENE company (Shanghai, China). For in vivo infection experiments, every mouse was intravenously administered AAV9-Sh$_{Scramble}$ and AAV9-Sh$_{Prkg1}$ with 2×10^{11}v.g. titer. Infection efficiency was analyzed in thoracic aorta samples by western blot.

Western Blot

Mouse tissues or cells were lysed in RIPA buffer (P0013B, Beyotime, Beijing, China) supplemented with protein phosphatase inhibitors (1:100). Protein concentrations were quantified using a BCA Protein Assay Kit (Thermo Scientific). Equal amounts of total proteins were resolved on 8% or 12% SDS-PAGE gels transferred onto nitrocellulose filter membranes (Pall, Port Washington, NY, USA). The membranes were blocked with 5% BSA and then incubated with the primary antibody and the IRDye 700/800DX-conjugated secondary antibody (Rockland Inc., Gilbertsville, PA, USA). The immunofluorescent signal was obtained using an Odyssey infrared imaging system (LI-COR Biosciences, Lincoln, NE, USA).

Cell Culture

Primary rat VSMCs were isolated from the thoracic aortas of 150 to 180 g male Sprague-Dawley rats by collagenase digestion. VSMCs were cultured in low glucose DMEM (Gibco) supplemented with 10% fetal bovine serum (FBS), 100 U/ml penicillin, and 100 μg/ml streptomycin. Primary VSMCs at passages 3 to 6 were used for all experiments. VSMCs were maintained at 37 °C in a humidified atmosphere with 5% CO_2.

TBAD study and Anatomical characteristics

TBAD clinical data is from the prospective multicenter clinical trial, conducted in accordance with the ethical standards of the Institutional Review Board of the Chinese PLA General Hospital (2020010), was carried out in 18 tertiary hospitals across China. The study was registered with ClinicalTrials.gov under the identifier NCT04765605.

For patient inclusion and exclusion criteria, we excluded deceased patients for whom CTA data could no longer be obtained and patients with major postoperative complications, such as stroke, respiratory failure, retrograde type A aortic dissection, re-intervention, stent-induced new entry, stent migration, stenosis or occlusion of the LSA branch stent, and spinal cord ischemia, due to their poor health status in subsequent follow-ups. In addition, several patients who were not hypertensive were also excluded from this study.

For antihypertensive medication, we confirmed and recorded the patients' use of antihypertensive medication through discharge medication records, subsequent follow-up information from outpatient visits at the central hospital, and telephone follow-ups.

For CTA measurements, briefly, a series of morphological parameters of TBAD were measured on the preoperative and postoperative CTA images. The measurement protocol strictly followed the reporting standards for TBAD recommended by the Society for Vascular Surgery and Society of Thoracic Surgeons[30]. All measurements were obtained using post-processing image software (3Mensio Workstation version 10.4, Maastricht, the Netherlands) that enabled aortic centre lumen line extraction and reconstruction. Aortic diameter was measured in three fixed planes, including: (1) 2 cm distal to the left subclavian artery (LSA); (2) the middle point of the descending thoracic aorta (DTA) and (3) the superior border of the celiac artery (CA). Additionally, the maximal diameter of the DTA was also recorded. Suggested by the Society for Vascular Surgery and Society of Thoracic Surgeons, the aortic diameter was measured from the outer aortic wall to outer aortic wall, and the diameters of the true lumen (TL) and false lumen (FL) on these four interested observed planes were simultaneously measured. The volumes of the DTA (Ishimaru zones 3-4 and zone 5) was also measured by using the "volume segmentation function" of the post-processing software 3Mensio Vascular. The descending thoracic aorta is anatomically divided into the Ishimaru zones 3-4 and zone 5 (Supplementary Fig. 4a).

Statistical analysis

For UKB data, we summarized the baseline characteristics of the study stratified by hypertension and CCBs use or other antihypertensive medication, or hypertension without antihypertensive medication use,

https://doi.org/10.1038/s41467-025-68086-5

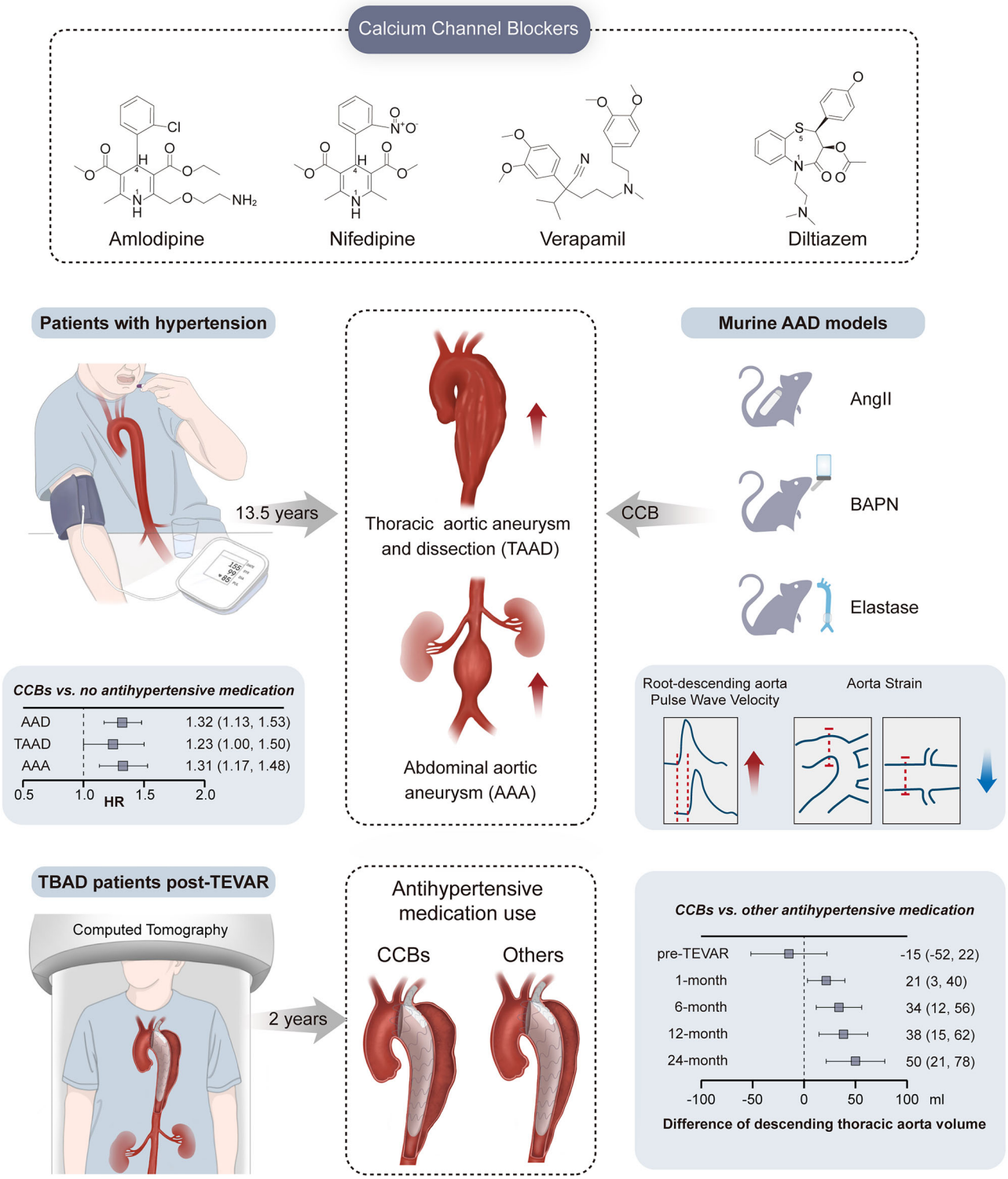

Fig. 8 | Summary diagram. CCB calcium channel blocker, AAD aortic aneurysm and dissection, TAAD thoracic aortic aneurysm and dissection, AAA abdominal aortic aneurysm, TBAD type B aortic dissection, TEVAR thoracic aorta endovascular repair.

or no hypertension (Fig. 1 and Supplementary Table 5). Person-time was calculated from the baseline to the occurrence of study outcomes, death, or the end of follow-up (October 31, 2022 [England], July 31, 2021 [Scotland], and February 28, 2018 [Wales]), whichever came first. Cox proportional hazards regression models were applied to examine the risk of AAD or AAD subtypes, adjusting for age, sex, BMI, total cholesterol, triglycerides, smoking status, education, ethnicity, and systolic blood pressure. Sensitivity analyses were conducted to minimize the bias: (1) a broader definition of hypertension was applied; (2) restricted to participants without coronary artery disease to address the issue that coronary artery disease might confound the association between CCBs use and AAD; (3) the Fine & Gray competing risk model to account for the presence of competing events (death from all causes except for AAD). We tested the proportional hazard assumption with

Schoenfeld residuals and did not detect any significant violation of this assumption. Among participants with hypertension, mixed-effects linear models with unstructured variance structure were used to analyze the effect of groups (without any antihypertensive medications, CCBs use, and other antihypertensive medications excluding CCBs use) on systolic/diastolic blood pressure, with participants treated as random effects, group, time (baseline or follow-up), and their interaction as fixed effects, adjusting for age, sex, BMI, total cholesterol, triglycerides, smoking status, education, ethnicity, and baseline systolic/diastolic blood pressure. Estimated marginal means and 95% CI were the adjusted values from the models and post hoc pairwise comparisons used Bonferroni correction. Statistical analyses for the UKB were performed using R version 3.6.3.

For experiments data, statistical analyses were performed using GraphPad Prism 8.0 software (San Diego, CA, USA). Data are expressed as mean ± SEM. The details of the statistical analysis used in each experiment are presented in the corresponding figure legends. For statistical comparisons, we first evaluated whether the data were normally distributed using the Shapiro Wilk normality test. For two groups, we used unpaired Student's *t* test for normally distributed data. If the data was skewed distribution, we used Mann-Whitney test. For more than two groups with one variable, we used one-way ANOVA followed by post hoc analysis for comparisons among normally distributed data. Specifically, Dunnett's multiple comparison test was used to compare each group with a control group, while Tukey's multiple comparisons test was used to compare each group with every other group. If the data equal variances were not assumed, Brown-Forsythe and Welch ANOVA test was used with Dunnett T3 multiple comparisons test (compare each group with a control group) or Games-Howell multiple comparisons test (compare each group with every other group). For more than two groups with two variables, we used two-way ANOVA (mixed model) among normally distributed data. Specifically, Dunnett's multiple comparison test was used to compare one variable within each another variable to control group. If the data equal variances were not assumed, Geisser-Greenhouse correction was used. Nonparametric tests (Kruskal-Walli's test) were used when the data were not normally distributed. In addition, Fisher's test was used for contingency data and Log-rank test was used Kaplan-Meier curve.

For human study, statistical analyses were performed using GraphPad Prism 8.0 software (San Diego, CA, USA) and SPSS Statistics 26 (IBM, NY, USA). Data are expressed as mean ± SEM or percentages. For statistical comparisons, unpaired Student's *t* test and χ test (Fisher's test) was used for the comparison of patient's baseline characteristics, CTA measurements and diameters or volumes growth rates at 1- or 2-year post-TEVAR. Mixed-effects model without adjustment was used to compare whether there are statistically significant differences in the trends of diameters and volumes between the two groups over a 2-year follow-up period. This model accounts for repeated measures within subjects and evaluates changes over time without adjusting for potential confounding variables. Furthermore, we applied a general linear mixed-effects model, adjusting for potential influencing factors, including age (years), sex (men; women), systolic blood pressure (mmHg), family history of cardiovascular disease (yes; no), diabetes (yes; no), hyperlipidemia (yes; no), coronary heart disease (yes; no), false lumen length grades (1-8), total false lumen thrombus score (0;1;2;3 levels for each zone and combined score for all zones), number of distal tears (zone 5-9), initial tear diameter (mm), and interactions of these factors with CCB use. We then compared whether the trends of diameters and volumes between the two groups over the 2-year follow-up period showed statistically significant differences. Additionally, we assessed whether the differences in diameter and volume between the two groups at preoperative and postoperative time points (1, 6, 12, and 24 months) were statistically significant.

In all analyses, P-value < 0.05 was regarded as statistically significant.

Reporting summary

Further information on research design is available in the Nature Portfolio Reporting Summary linked to this article.

Data availability

The UK Biobank datasets analyzed during the current study are available in a public, open access repository (https://www.ukbiobank.ac.uk/). The data are available for approved researchers through the UK Biobank data-access protocol. This research has been conducted using the UK Biobank resource under application number 96083. All data supporting the findings of this study are available within the article and its Supplementary Information files. Source data are provided with this paper. Additional raw data are available from the corresponding author upon request. Source data are provided with this paper.

Code availability

R codes for supporting UK Biobank analyses are deposited at: https://github.com/cookiemonsterxxm/CCBs_AAD.

References

1. Baman, J. R. & Malaisrie, S. C. What Is Aortic Dissection? *JAMA* **330**, 198 (2023).
2. Wanhainen, A. et al. Editor's Choice - European Society for Vascular Surgery (ESVS) 2019 Clinical Practice Guidelines on the Management of Abdominal Aorto-iliac Artery Aneurysms. *Eur. J. Vasc. Endovasc. Surg.* **57**, 8–93 (2019).
3. Pinard, A., Jones, G. T. & Milewicz, D. M. Genetics of Thoracic and Abdominal Aortic Diseases. *Circ. Res* **124**, 588–606 (2019).
4. Hameed, I., Cifu, A. S. & Vallabhajosyula, P. Management of Thoracic Aortic Dissection. *JAMA* **329**, 756–757 (2023).
5. Golledge, J. et al. Efficacy of Telmisartan to Slow Growth of Small Abdominal Aortic Aneurysms: A Randomized Clinical Trial. *JAMA Cardiol.* **5**, 1374–1381 (2020).
6. Siordia, J. A. Beta-Blockers and Abdominal Aortic Aneurysm Growth: A Systematic Review and Meta-Analysis. *Curr. Cardiol. Rev.* **17**, e230421187502 (2021).
7. Bicknell, C. D., Kiru, G., Falaschetti, E., Powell, J. T. & Poulter, N. R. An evaluation of the effect of an angiotensin-converting enzyme inhibitor on the growth rate of small abdominal aortic aneurysms: a randomized placebo-controlled trial (AARDVARK). *Eur. Heart J.* **37**, 3213–3221 (2016).
8. Pinchbeck, J. L. et al. Randomized Placebo-Controlled Trial Assessing the Effect of 24-Week Fenofibrate Therapy on Circulating Markers of Abdominal Aortic Aneurysm: Outcomes From the FAME -2 Trial. *J. Am. Heart Assoc.* **7**, e009866 (2018).
9. Sillesen, H. et al. Randomized clinical trial of mast cell inhibition in patients with a medium-sized abdominal aortic aneurysm. *Br. J. Surg.* **102**, 894–901 (2015).
10. Baxter, B. T. et al. Effect of Doxycycline on Aneurysm Growth Among Patients With Small Infrarenal Abdominal Aortic Aneurysms: A Randomized Clinical Trial. *JAMA* **323**, 2029–2038 (2020).
11. Karlsson, L., Gnarpe, J., Bergqvist, D., Lindbäck, J. & Pärsson, H. The effect of azithromycin and Chlamydophilia pneumonia infection on expansion of small abdominal aortic aneurysms-a prospective randomized double-blind trial. *J. Vasc. Surg.* **50**, 23–29 (2009).
12. Wanhainen, A. et al. The effect of ticagrelor on growth of small abdominal aortic aneurysms-a randomized controlled trial. *Cardiovasc Res* **116**, 450–456 (2020).
13. Hibino, M. et al. Blood Pressure, Hypertension, and the Risk of Aortic Dissection Incidence and Mortality: Results From the J-SCH Study, the UK Biobank Study, and a Meta-Analysis of Cohort Studies. *Circulation* **145**, 633–644 (2022).
14. Rapsomaniki, E. et al. Blood pressure and incidence of twelve cardiovascular diseases: lifetime risks, healthy life-years lost, and age-

specific associations in 1·25 million people. *Lancet* **383**, 1899–1911 (2014).
15. Humphrey, J. D., Milewicz, D. M., Tellides, G. & Schwartz, M. A. Cell biology. Dysfunctional mechanosensing in aneurysms. *Science* **344**, 477–479 (2014).
16. Ailawadi, G. et al. Smooth muscle phenotypic modulation is an early event in aortic aneurysms. *J. Thorac. Cardiovasc Surg.* **138**, 1392–1399 (2009).
17. Ostberg, N. P., Zafar, M. A., Ziganshin, B. A. & Elefteriades, J. A. The Genetics of Thoracic Aortic Aneurysms and Dissection: A Clinical Perspective. *Biomolecules* **10**, 182 (2020).
18. Milewicz, D. M. et al. Altered Smooth Muscle Cell Force Generation as a Driver of Thoracic Aortic Aneurysms and Dissections. *Arterioscler Thromb. Vasc. Biol.* **37**, 26–34 (2017).
19. Qian, W. et al. Microskeletal stiffness promotes aortic aneurysm by sustaining pathological vascular smooth muscle cell mechanosensation via Piezo1. *Nat. Commun.* **13**, 512 (2022).
20. Nolasco, P. et al. Impaired vascular smooth muscle cell force-generating capacity and phenotypic deregulation in Marfan Syndrome mice. *Biochim Biophys. Acta Mol. Basis Dis.* **1866**, 165587 (2020).
21. Nollen, G. J., Groenink, M., Tijssen, J. G., Van Der Wall, E. E. & Mulder, B. J. Aortic stiffness and diameter predict progressive aortic dilatation in patients with Marfan syndrome. *Eur. Heart J.* **25**, 1146–1152 (2004).
22. Nam, G. T-type calcium channel blockers: a patent review (2012-2018). *Expert Opin. Ther. Pat.* **28**, 883–901 (2018).
23. Kanematsu, Y. et al. Pharmacologically induced thoracic and abdominal aortic aneurysms in mice. *Hypertension* **55**, 1267–1274 (2010).
24. Mieth, A. et al. L-type calcium channel inhibitor diltiazem prevents aneurysm formation by blood pressure-independent anti-inflammatory effects. *Hypertension* **62**, 1098–1104 (2013).
25. Chen, X. et al. Amlodipine reduces AngII-induced aortic aneurysms and atherosclerosis in hypercholesterolemic mice. *PLoS One* **8**, e81743 (2013).
26. Kurobe, H. et al. Azelnidipine suppresses the progression of aortic aneurysm in wild mice model through anti-inflammatory effects. *J. Thorac. Cardiovasc Surg.* **146**, 1501–1508 (2013).
27. Doyle, J. J. et al. A deleterious gene-by-environment interaction imposed by calcium channel blockers in Marfan syndrome. *Elife* **4**, e08648 (2015).
28. in *LiverTox: Clinical and Research Information on Drug-Induced Liver Injury* (National Institute of Diabetes and Digestive and Kidney Diseases, (2012).
29. Regnault, V., Lacolley, P. & Laurent, S. Arterial Stiffness: From Basic Primers to Integrative Physiology. *Annu Rev. Physiol.* **86**, 99–121 (2024).
30. Lombardi, J. V. et al. Society for Vascular Surgery (SVS) and Society of Thoracic Surgeons (STS) reporting standards for type B aortic dissections. *J. Vasc. Surg.* **71**, 723–747 (2020).
31. Toral, M., de la Fuente-Alonso, A., Campanero, M. R. & Redondo, J. M. The NO signalling pathway in aortic aneurysm and dissection. *Br. J. Pharm.* **179**, 1287–1303 (2022).
32. Schwaerzer, G. K. et al. Aortic pathology from protein kinase G activation is prevented by an antioxidant vitamin B(12) analog. *Nat. Commun.* **10**, 3533 (2019).
33. Guo, D. C. et al. Recurrent gain-of-function mutation in PRKG1 causes thoracic aortic aneurysms and acute aortic dissections. *Am. J. Hum. Genet* **93**, 398–404 (2013).
34. Groenink, M. et al. Losartan reduces aortic dilatation rate in adults with Marfan syndrome: a randomized controlled trial. *Eur. Heart J.* **34**, 3491–3500 (2013).
35. Mullen, M. et al. Irbesartan in Marfan syndrome (AIMS): a double-blind, placebo-controlled randomised trial. *Lancet* **394**, 2263–2270 (2019).
36. Lacro, R. V. et al. Atenolol versus losartan in children and young adults with Marfan's syndrome. *N. Engl. J. Med* **371**, 2061–2071 (2014).
37. van Andel, M. M. et al. Long-term clinical outcomes of losartan in patients with Marfan syndrome: follow-up of the multicentre randomized controlled COMPARE trial. *Eur. Heart J.* **41**, 4181–4187 (2020).
38. Chiu, H. H. et al. Losartan added to β-blockade therapy for aortic root dilation in Marfan syndrome: a randomized, open-label pilot study. *Mayo Clin. Proc.* **88**, 271–276 (2013).
39. Shores, J., Berger, K. R., Murphy, E. A. & Pyeritz, R. E. Progression of aortic dilatation and the benefit of long-term beta-adrenergic blockade in Marfan's syndrome. *N. Engl. J. Med* **330**, 1335–1341 (1994).
40. Isselbacher, E. M. et al. 2022 ACC/AHA Guideline for the Diagnosis and Management of Aortic Disease: A Report of the American Heart Association/American College of Cardiology Joint Committee on Clinical Practice Guidelines. *Circulation* **146**, E334–E482 (2022).
41. Mazzolai, L. et al. 2024 ESC Guidelines for the management of peripheral arterial and aortic diseases. *Eur. Heart J.* **45**, 3538–3700 (2024).
42. Pitcher, A. et al. Angiotensin receptor blockers and β blockers in Marfan syndrome: an individual patient data meta-analysis of randomised trials. *Lancet* **400**, 822–831 (2022).
43. Tang, L. et al. Structural basis for inhibition of a voltage-gated Ca(2+) channel by Ca(2+) antagonist drugs. *Nature* **537**, 117–121 (2016).
44. Hockerman, G. H., Peterson, B. Z., Johnson, B. D. & Catterall, W. A. Molecular determinants of drug binding and action on L-type calcium channels. *Annu Rev. Pharm. Toxicol.* **37**, 361–396 (1997).
45. Triggle, D. J. Calcium channel antagonists: clinical uses-past, present and future. *Biochem Pharm.* **74**, 1–9 (2007).
46. Liao, S. et al. Suppression of experimental abdominal aortic aneurysms in the rat by treatment with angiotensin-converting enzyme inhibitors. *J. Vasc. Surg.* **33**, 1057–1064 (2001).
47. Liu, S. et al. Mineralocorticoid receptor agonists induce mouse aortic aneurysm formation and rupture in the presence of high salt. *Arterioscler Thromb. Vasc. Biol.* **33**, 1568–1579 (2013).
48. Sawada, H. et al. Inhibition of the Renin-Angiotensin System Fails to Suppress β-Aminopropionitrile-Induced Thoracic Aortopathy in Mice-Brief Report. *Arterioscler Thromb. Vasc. Biol.* **42**, 1254–1261 (2022).
49. Zhu, L. et al. Mutations in myosin heavy chain 11 cause a syndrome associating thoracic aortic aneurysm/aortic dissection and patent ductus arteriosus. *Nat. Genet* **38**, 343–349 (2006).
50. Guo, D. C. et al. Mutations in smooth muscle alpha-actin (ACTA2) lead to thoracic aortic aneurysms and dissections. *Nat. Genet* **39**, 1488–1493 (2007).
51. Wang, L. et al. Mutations in myosin light chain kinase cause familial aortic dissections. *Am. J. Hum. Genet* **87**, 701–707 (2010).
52. de Cárcer, G. et al. Plk1 regulates contraction of postmitotic smooth muscle cells and is required for vascular homeostasis. *Nat. Med* **23**, 964–974 (2017).
53. Zhang, C., Mohan, A., Shi, H. & Yan, C. Sildenafil (Viagra) Aggravates the Development of Experimental Abdominal Aortic Aneurysm. *J. Am. Heart Assoc.* **11**, e023053 (2022).
54. Yang, L. et al. Protein kinase G phosphorylates Cav1.2 alpha1c and beta2 subunits. *Circ. Res.* **101**, 465–474 (2007).
55. de la Fuente-Alonso, A. et al. Aortic disease in Marfan syndrome is caused by overactivation of sGC-PRKG signaling by NO. *Nat. Commun.* **12**, 2628 (2021).
56. Wilmink, A. B. et al. Are antihypertensive drugs associated with abdominal aortic aneurysms? *J. Vasc. Surg.* **36**, 751–757 (2002).
57. Raaz, U. et al. Segmental aortic stiffening contributes to experimental abdominal aortic aneurysm development. *Circulation* **131**, 1783–1795 (2015).

58. Humphrey, J. D. Vascular adaptation and mechanical homeostasis at tissue, cellular, and sub-cellular levels. *Cell Biochem Biophys.* **50**, 53–78 (2008).
59. Dajnowiec, D. & Langille, B. L. Arterial adaptations to chronic changes in haemodynamic function: coupling vasomotor tone to structural remodelling. *Clin. Sci. (Lond.)* **113**, 15–23 (2007).
60. Dai, C. & Khalil, R. A. Calcium Signaling Dynamics in Vascular Cells and Their Dysregulation in Vascular Disease. *Biomolecules* **15**, 892 (2025).
61. Yang, H., Raymer, K., Butler, R., Parlow, J. & Roberts, R. The effects of perioperative beta-blockade: results of the Metoprolol after Vascular Surgery (MaVS) study, a randomized controlled trial. *Am. Heart J.* **152**, 983–990 (2006).
62. Rašiová, M. et al. Positive association between calcium channel blocker treatment and persistent type II endoleak. *Int Angiol.* **41**, 277–284 (2022).
63. Kertai, M. D., Westerhout, C. M., Varga, K. S., Acsady, G. & Gal, J. Dihydropiridine calcium-channel blockers and perioperative mortality in aortic aneurysm surgery. *Br. J. Anaesth.* **101**, 458–465 (2008).
64. Railton, C. J., Wolpin, J., Lam-McCulloch, J. & Belo, S. E. Renin-angiotensin blockade is associated with increased mortality after vascular surgery. *Can. J. Anaesth.* **57**, 736–744 (2010).
65. Bastos Gonçalves, F. et al. Clinical outcome and morphologic analysis after endovascular aneurysm repair using the Excluder endograft. *J. Vasc. Surg.* **56**, 920–928 (2012).
66. Kim, W. et al. Effect of β-blocker on aneurysm sac behavior after endovascular abdominal aortic repair. *J. Vasc. Surg.* **65**, 337–345 (2017).
67. Alshaikh, H. N., Canner, J. K. & Malas, M. Effect of Beta Blockers on Mortality After Open Repair of Abdominal Aortic Aneurysm. *Ann. Surg.* **267**, 1185–1190 (2018).
68. Chen, S. W. et al. Effect of β-blocker therapy on late outcomes after surgical repair of type A aortic dissection. *J. Thorac. Cardiovasc Surg.* **159**, 1694–1703.e1693 (2020).
69. Nejim, B., Mathlouthi, A., Naazie, I. & Malas, M. B. The Effect of Intravenous and Oral Beta-Blocker Use in Patients with Type B Thoracic Aortic Dissection. *Ann. Vasc. Surg.* **80**, 170–179 (2022).
70. Chang, H. et al. Beta-blocker use after thoracic endovascular aortic repair in patients with type B aortic dissection is associated with improved early aortic remodeling. *J. Vasc. Surg.* **76**, 1477–1485.e1472 (2022).
71. Laio, K. M. et al. Prescription pattern and effectiveness of antihypertensive drugs in patients with aortic dissection who underwent surgery. *Front Pharm.* **14**, 1291900 (2023).
72. Elsayed, N., Gaffey, A. C., Abou-Zamzam, A. & Malas, M. B. Renin-Angiotensin-Aldosterone System Inhibitors Are Associated With Favorable Outcomes Compared to Beta Blockers in Reducing Mortality Following Abdominal Aneurysm Repair. *J. Am. Heart Assoc.* **12**, e029761 (2023).
73. Vicario-Feliciano, R., Zil, E. A. A. & Aziz, F. Beta Blockers are Associated with Increased Mortality Without a Decrease in Reinterventions After Endovascular Abdominal Aortic Repair (EVAR). *Ann. Vasc. Surg.* **110**, 395–404 (2025).
74. Deery, S. E. et al. Aneurysm sac expansion is independently associated with late mortality in patients treated with endovascular aneurysm repair. *J. Vasc. Surg.* **67**, 157–164 (2018).
75. O'Donnell, T. F. X. et al. Aneurysm sac failure to regress after endovascular aneurysm repair is associated with lower long-term survival. *J. Vasc. Surg.* **69**, 414–422 (2019).
76. Zekavat, S. M. et al. Elevated Blood Pressure Increases Pneumonia Risk: Epidemiological Association and Mendelian Randomization in the UK Biobank. *Med* **2**, 137–148.e134 (2021).
77. Kastner, A. et al. Calcium Channel Blocker Use and Associated Glaucoma and Related Traits Among UK Biobank Participants. *JAMA Ophthalmol.* **141**, 956–964 (2023).
78. Shen, Y. et al. Targeting cytokine-like protein FAM3D lowers blood pressure in hypertension. *Cell Rep. Med* **4**, 101072 (2023).

Acknowledgements

We thank Prof. Qingbo Xu from Zhejiang University for his valuable guidance on this study. We also thank Meihong Li and Enmin Xie for their assistance with the experiments. This research was supported by funding from the National Key R&D Program of China (2022YFA1302900 to W.K., 2024YFC2419000 to W.G.), the National Natural Science Foundation of China (NSFC 82230010 to W.K., 82070494 to W.G., 82473622 to X.G., and 82300544 to Z.Y.C.), China Postdoctoral Science Foundation (2025M771404 to Z.Y.C.), Science and Technology Project of Tianjin Municipal Health Commission (TJWJ2023QN116 to L.C.).

Author contributions

W.K., W.G., X.G., and Z.Y.C. conceptualized and designed the study. W.K., W.G., X.G., Z.Y.C. supervised the study. T.F.M., Z.Y.C., X.M.X., L.C., A.W., Z.S.Z., S.T.Z., Z.K.H., J.J.L., S.L., and J.S.G performed the experiments and analyzed the data. X.H.W., Y.F., F.Y., J.Z., L.X.W. and H.P.Z. provided valuable guidance on the study design and experimental procedures. T.F.M., Z.Y.C., X.M.X., and L.C. wrote the manuscript with input from all authors. T.F.M., Z.Y.C., X.M.X., and L.C. contributed equally to this work. All authors edited the manuscript and approved the final manuscript.

Competing interests

The authors declare no competing interests.

Additional information

Supplementary information The online version contains supplementary material available at https://doi.org/10.1038/s41467-025-68086-5.

Correspondence and requests for materials should be addressed to Xiang Gao, Wei Guo or Wei Kong.

Peer review information *Nature Communications* thanks the anonymous reviewers for their contribution to the peer review of this work. A peer review file is available.